Deposition of Iron Oxyhydroxide over Graphene/ZIF-12 Composite for Electrocatalytic Water Oxidation

A dissertation submitted to department of chemistry, Quaid-I-Azam University, Islamabad in partial fulfilment of requirement for the degree of

Master of Philosophy

In

Inorganic/Analytical chemistry

By

Waheed Iqbal

Department of Chemistry

Quaid-i-Azam University

Islamabad

2019

بسم الله الرحمن الرحيم

Dedicated to

My beloved parent

and

Brother

Table of Contents

Acknowledgements

First of all, I pay my gratitude to *Almighty Allah*, the Lord and Creator of heaven and earth. He is certainly the supreme of my life. All respects for His last prophet *Hazrat Muhammad (S.A.W)* who bestowed us the perfect code of life.

It was great honor for me to work under the kind supervision and guidance of *Dr. Muhammad Arif Nadeem* Whose personal interest, dedication, value able suggestion and provoking guidance made it possible to complete this task in time. He righteously fortified me in planning my work and helped at every stage of this research contribution. I would like to forward my thanks to chairman of the department of Chemistry *Prof. Dr. Shahid Hameed* and head of inorganic section *Prof. Dr. Amin Badshah* for providing the required facilities.

I am highly thankful to Dr. Sageer Abbas, Shiasta Abrahim, Maryam Batool, Waqas Ali Shah, Ijaz Hussain, Arslan Hameed and all my other lab fellows for proper guidance.

I am thankful to all friends for their admiration, care and faith. I can not finish without acknowledging my family. I desire to express gratitude to my parents for nurturing and encouraging me throughout my life. I am always indebted to my family for their unconditional and untiring love, support, encouragement, trust and faith. I am also thank full to my brother Naveed Iqbal for support and help in my education.

This study was not possible without help and support of my sincere.

Waheed Iqbal

Table of Figures

List of tables

List of Abbreviations

CA	Chronoamperometry
CPE	Controlled potential electrolysis
CE	Counter electrode
CNG	Compressed natural gas
DMF	Dimethylformamide
FTO	Fluorine dopped tin oxide
HER	Hydrogen evolution reaction
HRTEM	High resolution tansmission electron microscopy
LSV	Linear sweep voltammetry
MOF	Metal organic frameworks
OER	oxygen evolution reaction
RHE	Reversible hydrogen electrode
RE	Reference electrode
SEM	Scanning electron microscopy
TOF	Turnover frequency
TGA	Thermogravimatric analysis
TEM	Trasmission electron microscopy
WE	Working electrode
XRD	X-ray diffaraction
XPS	X-ray photoelectron spectrosacopy
ZIF	Zeolitic imidazole frameworks

Abstract

Developing the efficient electro-catalyst based on earth abundant elements is demanding for water oxidation reaction. In this study, composite materials consist iron oxyhydroxide (FeOOH), graphene and a cobalt based metal-organic framework (MOF-12) have been fabricated as electro-catalyst for the water oxidation reaction. The catalysts were synthesized by solvothermal process and characterized by various analytical techniques, such as powder X-ray diffraction (PXRD), thermogravimetric analysis (TGA), X-ray photoelectron spectroscopy (XPS), scanning electron microscopy (SEM), transmission electron microscopy (TEM) and energy dispersive X-ray analysis (EDX). The fully characterized materials were then subjected to water oxidation reaction. Under the optimal conditions, the synthesized electro-catalyst ($FeOOH_{0.5}$:$ZIF-12_{0.5}$/graphene) showed the onset potential 1.4 V Vs reversible hydrogen electrode in 0.5 M KOH solution at pH = 12. The electrocatalyst has shown a low over-potential value of 291 mV for the current density $10 mA/cm^{2.}$ The tafel slop was also measured as 78 mV/dec. The designed electrocatalyst demonstrated outstanding electro-catalytic properties for accelerating oxygen evolution reaction under alkaline conditions.

Chapter 1

1.1. Introduction

The whole world facing the problem of energy crises and pollution. The major sources of energy in recent era are fossil fuels which causes environmental pollution and the reservoirs are progressively decreasing[1]. Now a days the world 's growing thirst for crude oil is 1000 barrels which means about 2.5 litres a day per each person living on global world. The global energy consumption value is 13 terawatt (TW)[2]. How long can we manage to survive in future? The most important issue of 21st century is energy. So many entangled and vital questions that are called to answer. How can we fulfil the highest amount of per capita energy consumption? How we can progressively stop burning fossil fuels? Can scientist's discovery any source of energy which can replace fossil fuels? Can chemistry help in solving the energy problem before the depletion of fossil fuels? Can peoples living in poor areas advance their quality of life? As scientist we do have duty to contribute our research work on the future energy crises. As chemists we can help improving energy technologies and scientific approaches to solve problems of at its root[3].

1.2. The hydrogen economy:

"I believe that water will one day be employed as fuel, that hydrogen and oxygen which constitute it, used singly or together, will furnish an inexhaustible source of heat and light, of an intensity of which coal is not capable. Water will be the coal of the future."

Clearly, both energy and environmental problem will be solved if we replace oil with hydrogen[4].

The Water is rich source of hydrogen. One molecule of water contains two hydrogen atoms. Water is very stable molecule, so it is very difficult to produce the hydrogen from water[5]. Hydrogen abstracted from water by following ways,

- Water electrolysis.
- Photochemical water splitting[6].
- Photo electro water splitting[7].

Figure 1.1: Hydrogen Fuel Bus using the hydrogen gas as fuel obtained from water (reproduce from[8])

Water is very stable molecule, so it is very difficult to abstract the hydrogen from water. There is the need catalyst which makes the water splitting more feasible under ordinary conditions.

1.3. Electrocatalysis:

Type of catalysis in which the increase of the rate of an electrochemical reaction taking place on an electrode surface in a electrolytic solution by using a substance (catalyst)[9]. The force that drives electro chemical reactions is electricity. The electrocatalyst is a chemical substance that function at electrode surfaces or may be the electrode surface itself that modify and enhance the electrochemical reaction[10].

The electrocatalyst are two types based on the phase.

1.3.1. Homogeneous electrocatalyst:

In the homogeneous catalysis the catalyst and reacting species are in the same phase, may be gas or liquid. However, the liquid phase homogeneous electrocatalysis are more other than gas phase. For example, the electrocatalytic reduction of dissolve carbon dioxide into the carbon mono oxide, methane or formic acid it depends upon the number transfer of electron[11].

$$CO_2 + 2\,H^+ + 2\,e^- \longrightarrow CO + H_2O$$

2

In this reaction the carbon dioxide is dissolved in the specific solvent then the catalyst is also dissolved in the solvent and then catalytic activity is performed on the pot the potentiostate. All the reactant and catalyst are in the solution or same phase. So, this type catalysis is homogeneous catalysis.

$$2H_2O \longrightarrow O_2 + 4H^+ + 4e^-$$

Another example of homogeneous catalysis is oxidation of water using platinum pyridinium complexes[12]. The water molecule split into one molecule of oxygen, four proton and four electrons are produced which are further reduced into molecular hydrogen and this molecular hydrogen is used as fuel.

1.3.2 Heterogeneous electrocatalysis:

The type of electrocatalysis in which the reactant and catalyst are not same phase, in this type mostly catalyst does not soluble in the solvent containing reactant. The advantage of heterogeneous catalysis is reuse of catalyst again and again for production of commercial products. The catalyst is obtained in their original condition by filtration, scratching from the surface of electrode etc.

There are many examples of heterogeneous catalysis.

Proton reduction using nickel sulphide in 0.5 M H_2SO_4.

$$4H^+ + 4e^- \longrightarrow 2H_2 \qquad E= 0 \text{ V vs RHE}$$

1.4 Electrochemical reactions:

Electrochemical reaction are those reactions in which the electrons are exchange between two species one is electrode and second is substance present in the electrolyte. These reactions may be electrolytic or galvanic. In the galvanic reactions the current is generated and in electrolytic reactions the current is used to drive the reactions.

Example:

Electrolysis of water into oxygen and hydrogen.
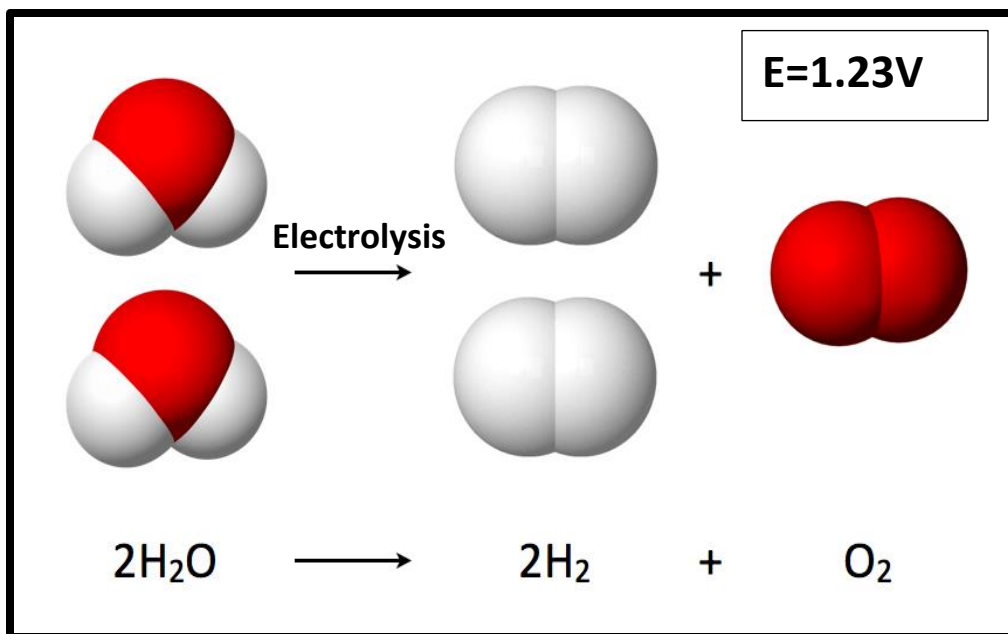
Figure 1.2: Electrocatalytic water splitting into hydrogen (white) and oxygen (red)

1.5. Electrolysis of water:

The electrolytic reactions consist of two half reactions one is oxidation and other is reduction. The half oxidation reaction electrons are produced due to oxidation of species and half reduction reaction the electrons are used to reduce the species[13]. Electro water splitting consist of two steps

1.5.1. Electro water reduction:

In electro water reduction four hydronium ion couple with four electrons to produce two molecules of hydrogen. The electro water reduction is thermo dynamically and Kinetically feasible reaction and requires very low potential for reduction.

$$4H^+ + 4e^- \longrightarrow 2H_2 \qquad E= 0 \text{ V vs RHE}$$

1.5.2. Electro water oxidation:

Water electrically oxidized in to oxygen molecule with four protons and electrons are produced. This reaction thermodynamically becomes feasible at 1.23 volts but kinetically sluggish. Water oxidation consist of more than one step, kinetics of each step is complex. The mechanism of electro water oxidation in acidic and basic medium is shown in the figure (1.3).
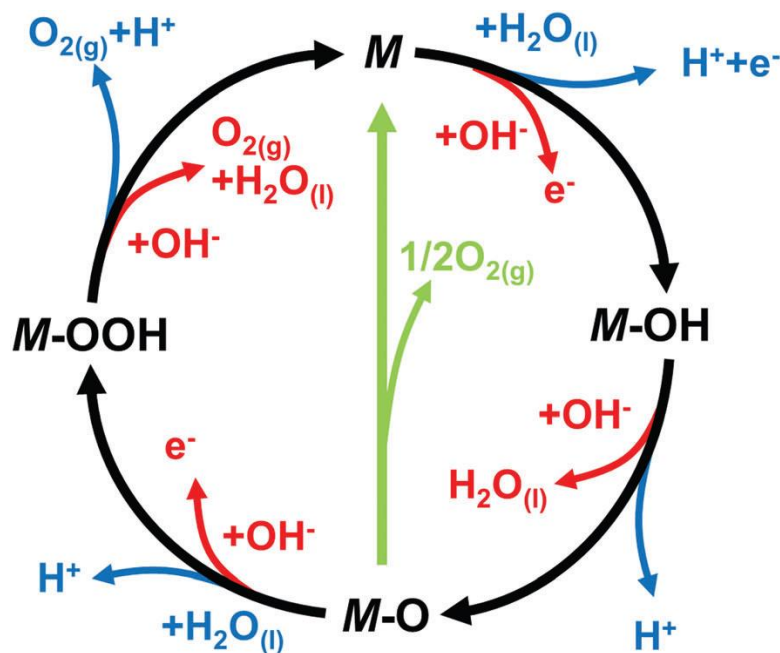
Figure 1.3: Mechanism of electro water oxidation in acidic and basic medium (reproduced from[14]).

So potential required other than thermodynamic potential for each step to make kinetics of reaction feasible[14].

$$2H_2O \longrightarrow O_2 + 4H^+ + 4e^- \quad E= 1.23 \text{ vs RHE}$$
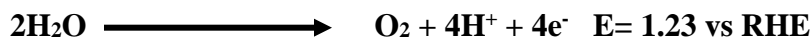
1.6. Oxygen evolution electrocatalyst:

Electrocatalyst for oxygen evolution are mostly noble metals (e.g, Au , Pt, Ir, Rh, Ru, Ag) but their oxides are more efficient toward OER than the corresponding metals[15]. Platinum shows good catalytic performance towards electro oxygen reduction reaction but weak activity towards OER, probably due to the formation of poor conductive monoxide layer during OER.

The volcano plot shows relationship between overpotential and enthalpy of adsorption. The transition metal oxides existing at the top of volcano plot showing the minimum overpotential and maximum catalytic activity. Heat of formation of substrate and attacking specie complex is intermediate at that point.
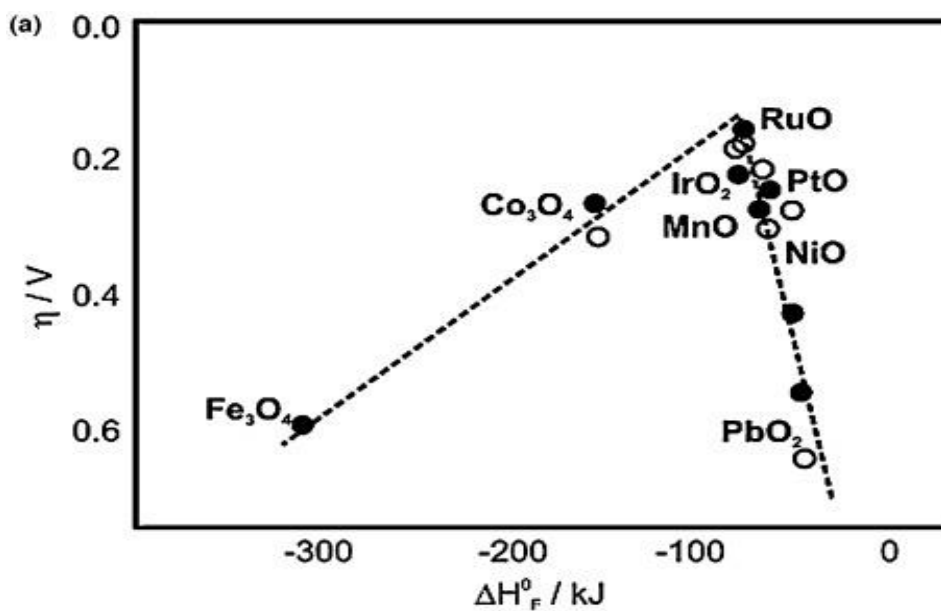
Figure 1.4: Volcano plot of metal oxide activities for electro water oxidation (reproduced[16])

Ruthenium and iridium forms oxides which are conductive and therefore find use as electrocatalyst toward oxygen evolution reaction. Ru-O is the best catalyst for oxygen evolution. But thermodynamically unstable due to the formation of higher valent oxides of Ru, thus resulting on formation of corrosion products at higher values of oxidation potential. In contrast the oxides of Ir exhibits strong resistance to corrosion during electro oxidation reaction but their activity is lower than Ru. The oxides of first row transition metals, mostly of cobalt and nickel shows efficient catalytic activity towards OER. But their oxides cause corrosion hence their use is restricted. Complex oxides based on Fe, Ni and Co are considered as active electrocatalyst for OER in alkaline medium[17].

Catalyst based on nanostructure architecture have been extensively used to study OER. The size of particle and shape of catalyst determine the activity of catalyst towards oxygen evolution[18]. Krtilet *al…* have studied the oxides of Ru, Co, Ni and their alloys with respect to the effect of size and shape of the catalyst in acidic solutions. The results of their experiments that revealed that crystal edges on the prismatic portion (the portion that reflects the light as prism) of RuO_2 are responsible for recombination of oxygen on these active sites. The activity of catalyst towards OER is independent of the size of particle but is affected by adding metals like Co and Ni[19].

Tilly et al[20], emphasized the size dependence of the crystalline nanoparticles of Co_2O_3 for their electrocatalytic behaviour towards OER in alkaline media. Nocerate.al electro deposited cobalt nitrate in phosphate buffer solution that showed excellent activity towards oxidation of water in neutral and mild conditions. The cobalt phosphate buffer was found to have a self-repair mechanism involving deposition / dissolution of ions of cobalt during oxidation of water. Ni borate buffer solution deposited on semiconductor materials such as FTO and ITO were also found useful for water oxidation under mild condition[21].

1.7. Thermodynamic of electrode reactions:

In the electrolysis primary energy input is the difference in potential between two electrodes. In electrochemical reactions involves the transfer of electrons between two electrodes and reactants and rate of this transfer can be tuned with ΔU the electrodes are immersed in the electrolyte which provides conductivity of ions due to high concentration of cations and anions. As the electrochemical reactions are redox reactions, therefor they can be divided into two half reaction, occurring at respective electrodes[22]. The change in Gibbs free energy of formation, determines the equilibrium potential (Ucell) according to the equation given below.

$$Ucell = -\Delta G/nF$$

The change in Gibbs free energy varies with temperature and pressure. This variation can be calculated for a general equation.

$$\Delta G = \Delta G° - RT\ln\frac{\alpha K}{\alpha mM}$$

Where G° represent the change in Gibbs free energy under standard condition, R is the general gas constant, T is the absolute temperature and a present the activity of reactants.
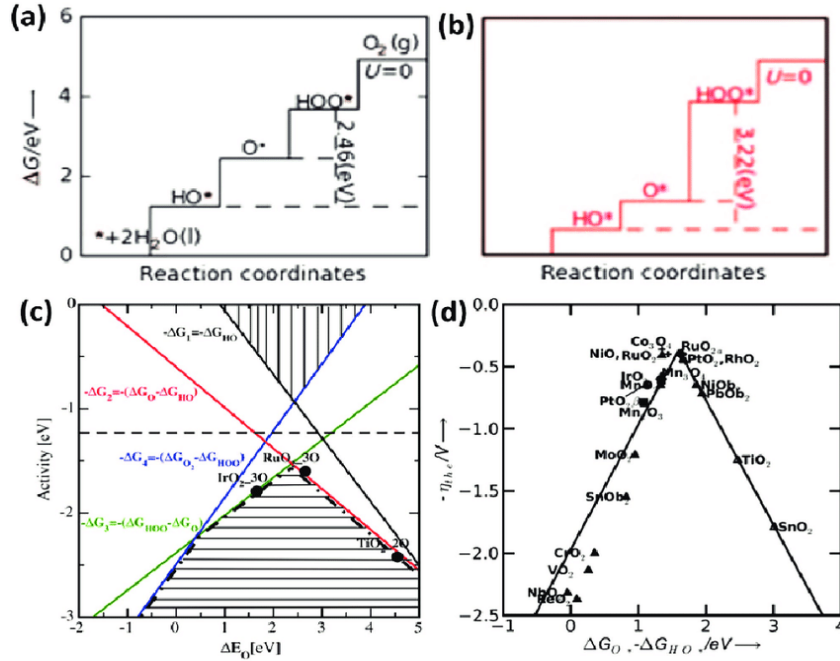
Figure 1.5: The relationship between Gibbs free energy and intermediate species in OER mechanism (reproduced[14])

The Nernst equation which gives relation of open circuit potential with temperature and pressure

$$U_{cell} = U°_{cell} – RT/nF \ln(a^j_J. a^k_K/a^m_M)$$

With the above mention equation, it is possible to evaluate the potential difference which is needed to run a spontaneous or a nonspontaneous reaction respectively in an electrochemical cell. However, the actual operating potential ΔU of such cell is significantly different from Ucell. The component of U is given in the following equation

$$U_{cell} = U°_{cell}±\eta±\Delta U_\Omega±\Delta U_t$$

In the equation ± tells the spontaneity of the reaction, if the value is + the reaction will be nonspontaneous and if its value – then reaction will be spontaneous. The symbol η represent the over potential, which need to drive the reaction when current is flowing due to non-ideal kinetics at the electrode surface. The ΔU_Ω represent the loss of potential due to resistance losses in the system and U_t donates the variation of potential with time. The research for electrolysis of water is concerned with finding the electrocatalyst with lower overpotential, high current density and

low Tafel slope. The theoretical expression between overpotential and current density is offered in the form of Butler Volmer equation.

$$j=j°[exp^{(1-\alpha)nF\eta/RT} - exp^{\alpha nF\eta/RT}]$$

Where $j°$ is the exchange current density and α is the symmetry factor. The j is a quantity which represent the current flowing both direction when the reaction is equilibrium. It is evident from the above equation that current exponentially depends overpotential. In the semi-logarithmic form this equation becomes the Tafel equation. Tafel equation is the simple form of Butler Volmer equation. Comprehensively, Tafel slope gives the relation between current density and overpotential. Tafel slope is another parameter to check the electrocatalytic activity of the catalyst. Tafel slope gives the change in potential for a ten- fold in current. Simply means, if the value of Tafel slope is low the electrocatalytic activity of catalyst will be high. Mostly Tafel slope has been used to check the mechanism of reaction and number of transfers of electron in the reaction. The value of Tafel slope is one to thirty, reaction will be one electron transfer, from thirty to sixty the reaction will be two electron transfer reaction. So, it tries lowering the overpotential as well as Tafel slope for electrocatalyst.

1.8. Role of solid support in catalysis:

Support is a material which provide the high surface area may enhance the conductivity of deposited material. In the heterogeneous catalysis the active centres are the metal atoms so there need much exposure of metal atoms to the reactant species[23]. This exposure of metal atoms increases by supporting the active sites over the specific surface increasing material which may be carbon, oxides of silicon, aluminium, titanium, calcium, magnesium and zinc. The catalyst supports are chosen according to the requirement of reaction.

Recent era much importance given to use carbon as support due to their high surface area, high conductivity, tuneable porosity, thermal, electrical and mechanical stability[24].

1.8.1. Carbon as a catalyst support:

Among many interesting applications, carbon and graphite materials considered for their utilization in several process involving heterogeneous catalytic reactions. Most of these consist of a metal or metallic compound with carbon as a support, the role of which is not only to keep the

catalytic segment in a well isolated conditions but also affect the catalytic activity by increasing the conductivity of the metal or supported material[25]. Their interaction and participation with active phase make catalyst supports more than just simple active phase carriers. Carbon is used as support since it has inertness towards unwanted reactions, stability, reasonable mechanical properties, reasonable conductivity, tuneable surface properties and porosity[26].

Carbon has a lot of application as support including hydrogenation of halogenated nitro aromatic chemicals and hydrogenation of alkene and alkynes, oxidation of organic compounds, and organic pollutants, carbon dioxide reduction, hydrogenation of carbon monoxide, in electro water oxidation and electro water reduction. The large-scale synthesis of vinyl acetate, vinyl chloride, and desulfurization of natural gas on activated carbon impregnated with ZnO, FeO, or CuO are important technical applications[27]. More recently, it has attained high attention with discovery of fullerenes in 1985 and the first HR-TEM observation of carbon nanotubes in 1991. Their use has been increased since separation of single layered graphene in 2002.

1.8.2. Activated carbon:

Activated carbon also called the activated charcoal and having the a lot of application in heterogeneous applications including Pt/C used in the fuel cell[28], used as support in the electro and photo splitting of water. While preparing activated carbon nanoparticles importance is given to increase the surface area, mechanical strength, high porosity[29] so that density of pi- sites present on partly graphitized structure is obtained[30]. Main applications of activated carbon supported catalyst in the industry are hydrogenation reactions that are important for pharmaceutical as intermediate and vitamins.

1.8.3. Graphite and graphitized materials:

Graphite has ability to form substituted graphitic material which having the high surface area, reasonable conductivity after specific temperature treatment. This substituted graphite was used for synthesis of thermally expended graphite material by chemical and electrochemical means with nitric or sulfuric acid[31]. Such material having high surface area ($100-400 cm^2/g$) being used as catalyst support.

1.8.4. Graphene as a Carbo catalyst

The use of heterogeneous carbon materials for the transformation or synthesis of organic or inorganic substrates are typically termed as carbocatalysts. Recently, the utilization of metal free catalysts supported carbonous materials attracting an excellent deal of interest[32]. Graphene primarily based materials like graphene compound (GO) are thought-about as a replacement category of carbocatalysts and opened a series of novel application prospects in chemical synthesis[33].
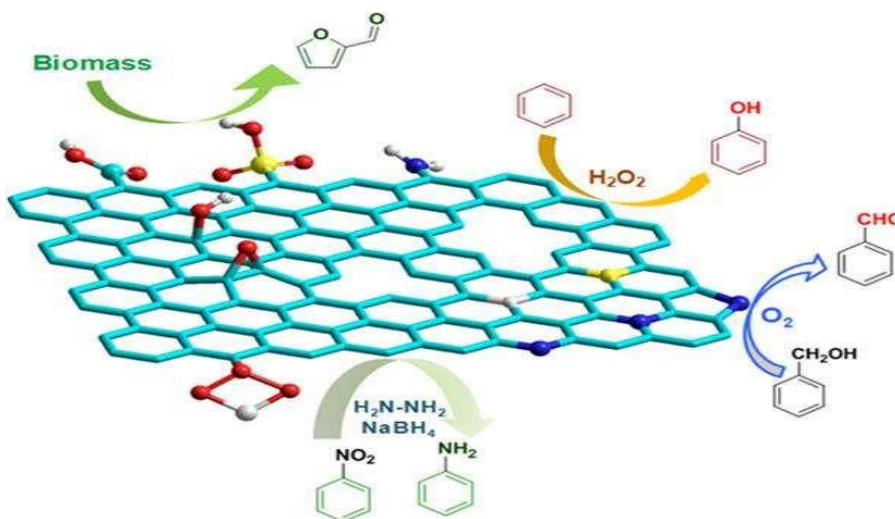
Figure 1.6: Graphene as carbo catalyst for degradation of nitrobenzene (reproduced from[34])

Since, Bielawski and colleagues[34] incontestable the power of graphene-based materials to facilitate variety of synthetically helpful transformations, the conception of "carbocatalysis" being wide explored and regarded as associate degree intriguing new direction in chemistry and materials science. The surface sure ventilated practical teams on the aromatic scaffold of GO is believed to permit ionic and non-ionic interactions with a good vary of molecules. varied transformation, as well as the oxidation of alcohols and alkenes into their several aldehydes and ketones, additionally because the association of alkynes have applied using graphene as a carbocatalyst. Recent reviews by Garcia et al[35]   and Loh et al.[36] comprehensively accounted a recent progress within the field of graphene enabled carbocatalysis. It's determined that the associate with myriad element atoms on its surface will perform as associate degree economical oxidizer throughout anaerobic oxidation and bear reduction at the tip of the primary chemical process cycle. Moreover, reduced graphene

oxides with its residual ventilated species still activate molecular element throughout aerobic oxidation.

1.8.5. Graphene as a Catalyst Support

In addition to their activity as a carbocatalyst, graphene primarily based materials are wide used as supports for catalytically active transition metals. excessiveness of reactions is being catalysed using totally different metal nanoparticles[37]. However, some obstacles are remaining like irreversible aggregation throughout electrocatalytic cycles, resulting in a major loss of nanoscale catalytic effect. Hence, proper catalyst support required to preserve the intrinsic surface properties. attributable to their extraordinarily high specific surface area that improves the dispersion of the catalytic metals, improved chemical and electrochemical stability at operation temperatures, increased electronic physical phenomenon, graphene primarily based materials are appealing selection as catalyst support.
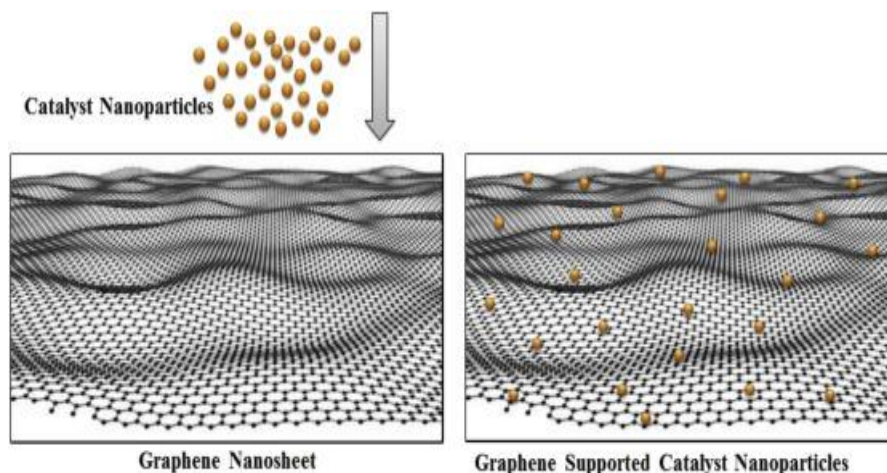
Figure 1.7: Nano particles supported on graphene used as catalyst (reproduced from[38])

Hence, graphene offers an ideal platform for catalytic molecular engineering. In one such example, Kim and colleagues[39] incontestable that gold nanoparticles (Au NPs) distributed on graphite oxide were able to turn alcohol oxidation. It's incontestable that the GO nanosheets not solely function structural parts of the multilayer thin film, however, conjointly doubtless improve the use and dispersion of Au NPs by taking benefits of the high catalytic area and therefore the electronic conductivity of graphene nanosheets. Similarly, graphene has been used as a support for numerous

metal oxides (ZnO, TiO_2, MnO_2, Fe_2O_3, Co_2O_4, etc)[40] and nanoparticles (Pt, Pd, Ag, Au or alloys)[41] to fabricate stratified catalyst systems.

1.9. Application of FeOOH and MOFS in Electrochemistry:

1.9 .1 Role of Iron Oxyhydroxide:

Recently, as one of the most vital transitional-metal-based Nano catalysts iron oxy-hydroxides (FeOOH) with open structure, low cost, natural abundance, and environmental friendliness of iron are step by step acknowledged and more explored for OER application[42]. However, the poor electrical conductivity of the FeOOH ($\sim 10^{-5}$ S cm^{-1}) remains a serious challenge and limits its mass-transfer kinetics. Thus, recently, some studies have tried to handle this issue by forming hybrid FeOOH nanomaterials

Solvothermal method is extensively used to produce new nanomaterials that requires specific chemical, physical and machinal properties. This method is popular in industries because of its simplicity and low cost in comparison to other method of synthesis. Therefore, using easily available comparatively cheaper element we synthesized Fe-Co based bimetallic electrocatalyst and investigated up water splitting process. It can be seen that price values of all the two transition metals being used in the work is lower than the commonly used other metals.

Table 1: Relative Prices of metals

Sr No	Metals	Price (per g) in USD
1	Pt	46.30
2	Pd	43.9
3	Ir	26.70
4	Ru	37.94
5	Co	2.1
6	Fe	3.1

The transition metal oxyhydroxides are oxide like material in which metal exist in 3+ oxidation state[43]. Mostly late transition metal like Mn, Iron, Co and Ni forms the oxyhydroxides. The main

properties of the oxyhydroxides these exist in layer form. The oxyhydroxides first was used in batteries as electrolyte in 1970s. Generally MOOH shows high electrocatalytic activity towards oxygen evolution activity[14]. In the oxyhydroxides protons are sandwiched between the layer of crystal structures and metal is present in the centre of the octahedron. These materials exist the different forms like α, β and γ depends upon the spaces between the layers[44]. Increasing trend towards the electro water oxidation the MOOH has been investigated the most active class for the reactions. Subbaraman et al[45] have confirmed the activity trend of transition metal oxyhydroxides (Ni>Co>Fe>Mn)[46]. However, the reason behind the activity is M-OH bond strength, the Ni shows the optimal bond strength and having the superior activity towards the oxygen evolution reactions according to Sabatier. However, Corrigan[45, 47] has been investigated the Fe impurity effect on the electrocatalytic activity of NiOOH[48]. The iron drops the overpotential up to 200mV. Later on, proved that Fe is the major catalytic site in this material.

The FeOOH are electroactive compound for the oxidation of water but limited use due to very poor conductivity[49], very small surface area and change into iron oxide anion at high voltage in basic media[50].
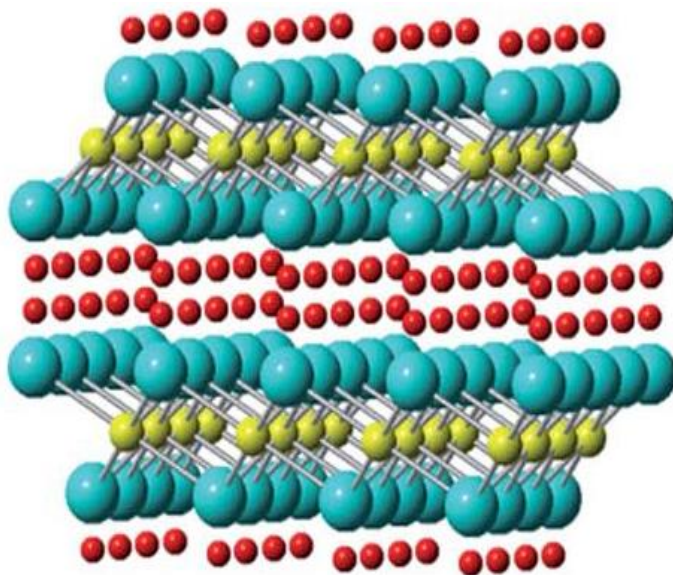
Figure 1.8: Structure of Iron oxyhydroxide showing (blue – oxygen, red – hydrogen yellow-iron) reproduced from[50a]

However, under high anodic potential the conductivity is increased but stability decreases. Here the electrocatalytic activity has been increased by supporting the iron oxyhydroxide over ZIF-12

and graphene[51]. Both he supports enhance the surface area and electrical conductivity which decrease the overpotential reason able.
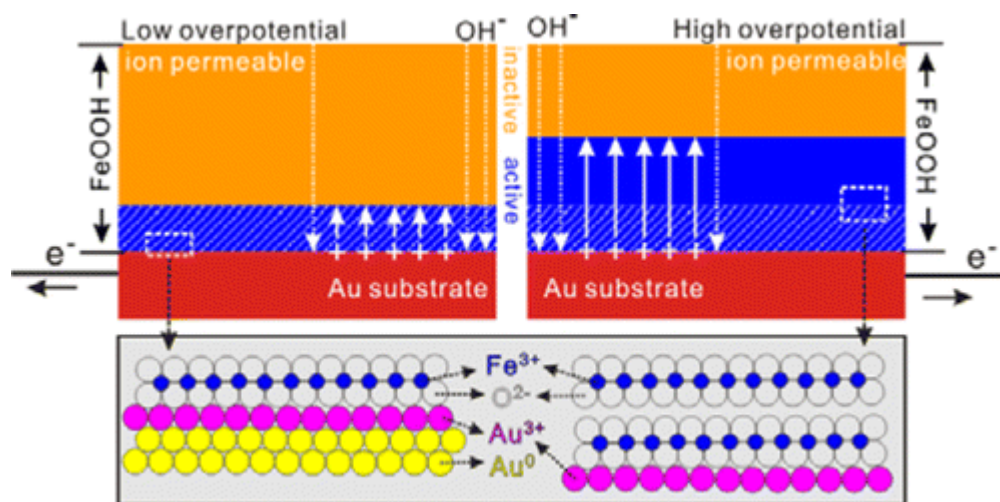
Figure 1.9: Showing the band gap relationship with conductivity of FeOOH (reproduced from[52])

1.9.2. Metal Organic Frameworks (MOFs):

Metal-organic frameworks (MOFs) are prepared by linking inorganic and organic units by robust bonds (reticular synthesis). Flexibleness with that the constituents' geometry, size, and practicality may be varied has junction rectifier to quite twenty thousand (20,000) completely different MOFs being reported and studied among the past decade[53]. To date, MOFs with permanent consistence are additional intensive in their selection and multiplicity than the other category of porous materials[54]. These aspects have created MOFs ideal candidates for storage of fuels (hydrogen and methane), capture of carbonic acid gas, and chemical process applications, to say some.

Porous materials have received enduring interest in natural science due to their quality for several applications, as well as host materials for molecular separation and storage, catalysis, molecular sensing, magnetism, and drug delivery systems.
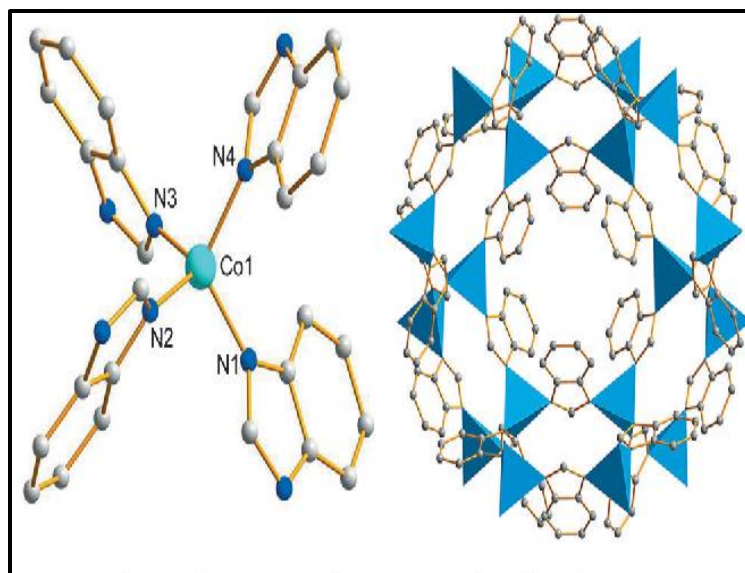
Figure 1.10: Structural composition of ZIF-9 which consist of cobalt and imidazole (reproduced from[55])

These porous solids are generally classified into 2 major categories: (i) amorphous and (ii) crystalline[56]. Porous amorphous solids (e.g., plastics, gels) don't exhibit any ordered continual units at intervals their structures, however it's helpful to figure with them as they're sometimes more cost-effective and simpler to organize. Their primary disadvantages are the possibly wide selection of molecular architectures with nonpredictable channels or topologies and also the lack of long-range order that leads to low mechanical stability. In distinction, the porous crystalline solids are a lot of advantageous thanks to their ordered structures with duplicatable pores/channels and topologies, that provide them high thermal and mechanical stability[57]. Nanoporous silicon dioxide and zeolites are characteristic samples of such ordered porous solids that have certain structural options with duplicatable pores/channels, dimensions, and topologies. These porous solids are divided into three classes supported their pore size. in step with the International Union of Pure and Applied Chemistry, the porousness of crystalline solids is typically given by the diameter of the pore size and is classified as microporous (5–20 Å), mesoporous (20–500 Å), and macro porous (>500 Å)[58].

1.9.3. Application of MOFs:

The high surface areas, tuneable pore metrics, and high density of active sites inside the terribly open structures of MOFs provide several benefits to their use in catalysis. MOFs may be wont to

support homogenized catalysts, stabilize transitory catalysts, perform size selectivity, and encapsulate catalysts inside their pores[59].
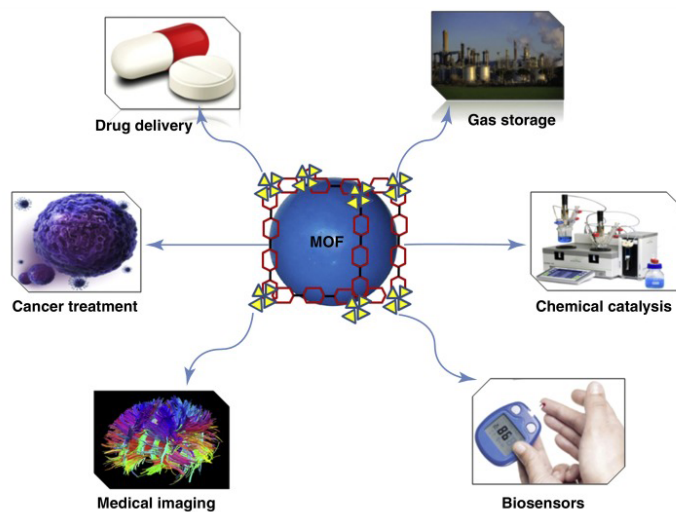
Figure 1.11: Applications of MOF in different fields (reproduced from[60])

MOFs are wide thought of as promising novel adsorbents for gas storage and separation because of their high surface areas, tune able pore size and structures, and versatile chemical compositions. element is taken into account to be one among the most effective different fuels to fossil fuels because of its high energy density, non-polluting combustion product, and natural abundance[61]. However, H_2 is a very volatile gas under ambient conditions, leading to a volumetrically energy density that's a lot of too low for sensible applications[62]. The goal thus is to design light-weight materials that may reversibly and quickly store H_2 close to ambient conditions at a density up to or bigger than liquid element. MOFs have attracted goodish attention within the H_2 cargo area in recent years thanks to their high operating capacities.

Natural gas, that consists chiefly of CH_4, is wide utilized as feedstock for synthesis gas in several countries. it's presently holds on as compressed gas (CNG) at 207 bar in pressure vessels, requiring a fashionable time period compression. a horny different to CNG is adsorbate gas (ANG), in, that the gas is hold on as Associate in Nursing adsorbate introduce a porous solid at a lower pressure. to market the conveyance application of methane series, the U S. DOE has set the target for methane series storage at a hundred and eighty V(STP)/V below thirty-five bar, close to close temperature, with the energy density of National Guard being cherish that of CNG presently used. a perfect material for CH_4 sorption ought to haven't solely an oversized accessible expanse

however conjointly an oversized pore volume, an occasional framework density, and powerful energetic interactions between the framework and CH_4 molecules.

Pervious work done on the electrocatalytic water oxidation has been shown in the table.

Table 1: Comparative activities of electrocatalysts in different electrolyte and substrate

Catalyst	Electrolyte	Substrate	Over potential (mV)	Tafel slope mV/dec
RuO_2	0.5 M KOH	FTO	$358@10 \ mA/cm^2$	55
IrO2	$0.5 \ H_2SO_4$	Ti	$290@ \ 1 \ mA//cm^2$	58
LaFeO3	1M KOH	FTO	$900@40 \ mA//cm^2$	88
CoFe2O4	0.1 M KOH	GCE	$390@10 \ mA//cm^2$	82
MnOOH	1M KOH	FTO	$556@10 \ mA//cm^2$	43
FeOOH	1M KOH	FTO	$525@10 \ mA//cm^2$	130
CoOOH	1M KOH	FTO	$475@10 \ mA//cm^2$	74
NiOOH	1M KOH	FTO	$350@10 \ mA//cm^2$	59
NiFe-LDH	1M KOH	FTO	$300@10 \ mA//cm^2$	43
NiCo-LDH	1M KOH	GCE	$335@10 \ mA//cm^2$	48
FeNi–rGO LDH	1M KOH	Ni Foam	$190@10 \ mA//cm^2$	39.5

1.10. Water splitting and contribution of present work:

Catalytic splitting of water provides an attractive potential solution to produce energy without polluting the environment using renewable energy sources. Synthesis of efficient, cost affordable and renewable catalysts and its implementation for a four electron transfer catalytic system at higher efficiency for OER/HER with moderate overpotential and high current density are the major challenges in this field. A key issue is to device a catalyst that exhibits a consecutive proton

coupled electron transfer regime during multi-electron water oxidation process. It should be able to separate the respective ions from water to produce oxygen with high rates and sustain its stability from many cycles. In addition, the available non-renew resources-based oxygen evolving assemblies perform water splitting at higher value of overpotential and lower current density that limit their applications in fuel cells. Therefore, the aim of this dissertation is to construct and explore environmentally friendly, cost affordable robust reusable and highly efficient electrocatalyst for the generation of energy from water splitting. The aim also to synthesize those catalyst which are highly stable in the alkaline medium at the high voltage to produce the maximum oxygen. The preparation of electrocatalyst involving synergetic properties enhancement of two metals is so far an unexpected explored material and interestingly its OER results are the best among all the reported water splitting catalyst used in literature.

CHAPTER 2

Experimental

This chapter includes chemicals, instrumentation and procedure used for the synthesis of electrocatalyst.

2.1. Materials and methods:

All chemicals and solvents used for synthesis were of analytical grade and used without further purification. The solutions required for coating purpose of FTO and electrochemical analysis of the sample were prepared in de-ionized water having resistivity of 18mΩ. The FTO coated film were prepared by using drop coasting method.

2.2.1. Synthesis of Iron oxy-hydroxide:

Iron oxy-hydroxide was synthesized by using the hydrothermal method. The iron trichloride hexahydrated (420mg) was dissoved in the de-ionized water, than the pH of the solution was increase upto 10.5 by adding the ammonium hydoxide (NH$_4$OH) drop wise and at the end sodium nitarte is added in the solution, the whole mixture was stirred for 20 minuts than whole mixutre was transferred in the 20mL teflon autoclave. The taflon autoclave was sealed for 24h at 140˚C. The autoclave cooled down to room temprature. The yellow crystals were obtained by centifugation, than washed with de-ionized water three times and dried at 70 ˚C for 24 hours.
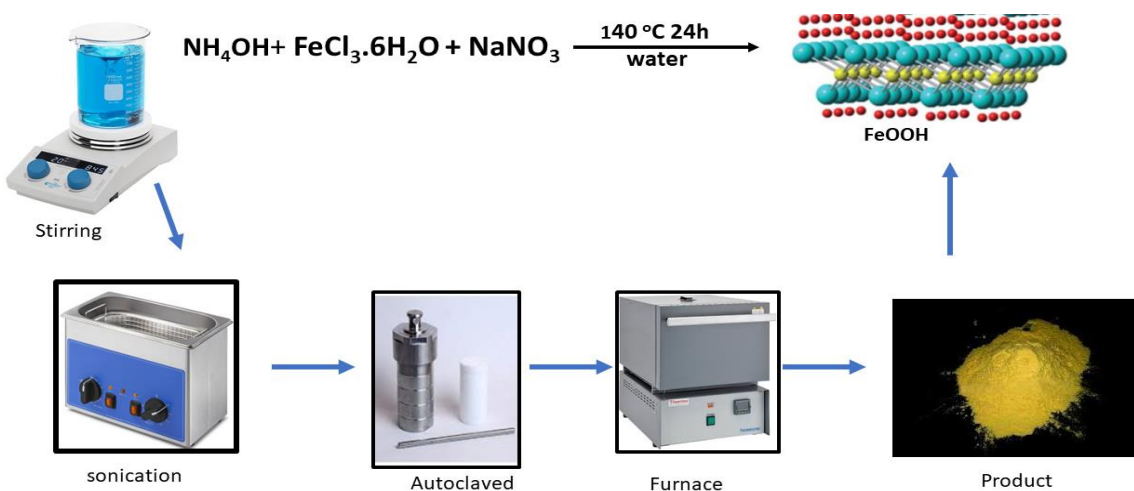

Figure 2.1: Systmatic diagram of synthesis of iron oxy hydroxide by hydrothermal method

2.2.2. Synthesis of FeOOH graphene composite:

The graphene based composite was synthesized by using the hydrothermalmethode. The 100mg graphene was dispersed in the aqueous solution of iron trichloride (100mg) and sodium nitrate by sonication for 4 hours and stirred for I hour. The blackesh yellow product obtained by filtration and product was washed by distil water and ethanol. Then obtained crystalline product vaccum dried at 80 °C for 8 hours. The graphene iron oxy-hydroxide based composites were synthesized with 1:1, 3:1 and1:3 respectively by applying the same hydrothermal method.

2.2.3. Sysnthesis of ZIF-12:

The zeolitic imedazolate frameworks were synthesized using the solvothermal method. The 420mg of cobalt nitrate hexahydrated ($Co(NO_3)_2$) and 720mg of benzimedazole were dissolved separately in the 7mL of dimethyl suformamide. Both the solutions were mixed and stirred vigorosly than whole solution was transferred into stainless steel autclave. The autoclave fixed in the ovan at 150 °C for 48 hours than autoclave cooled down to room temprature. The product was obtaind by filtration and washed three times with ethanol and dimethyl suformamide. The final product was vaccum dried at 120 °C over night.
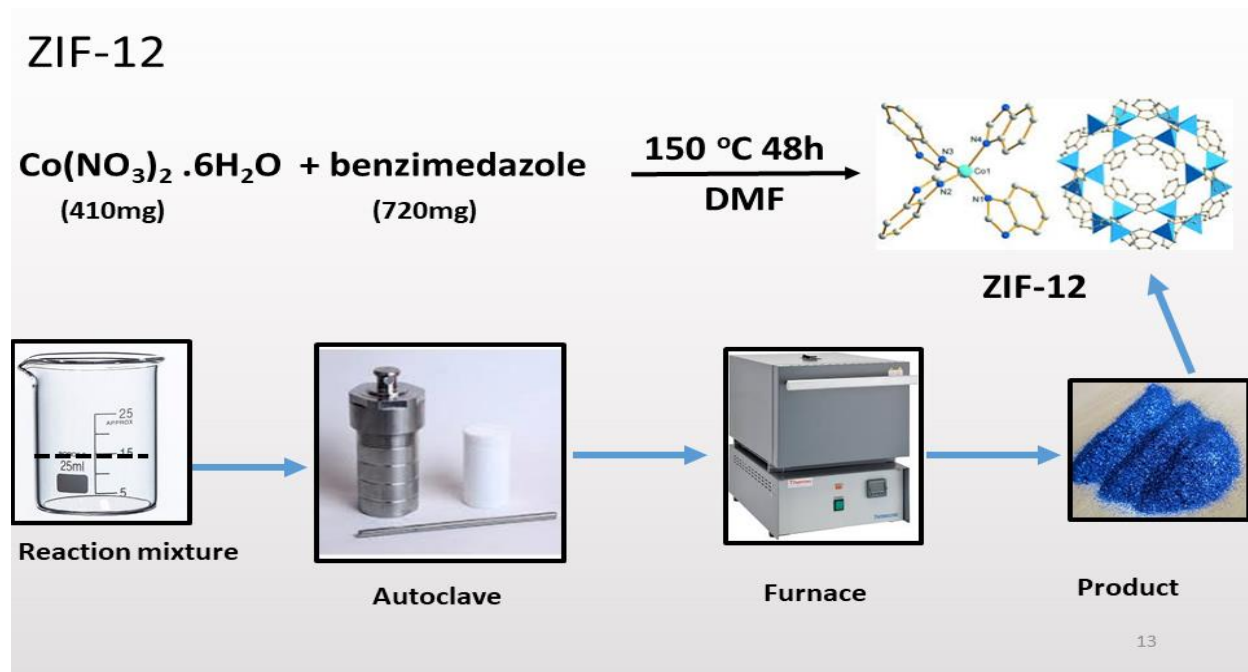
Figure 2.2: Systmatic diagram of synthesis of ZIF-12 by salvothermal method

2.2.4. Synthesis of Composite (FeOOH-graphene/ZIF-12) :

The final composite was also synthesized by using the hydrothermal technique. The graphene and pre synthsized MOF were dispersed in the aqeous solution of iron trichloride and than the whole

mixture was sonicated for three hours. Finally homogeneoied mixture was autoclaved at 140 ˚C for 24 hours. The bleckish green product was obtained by filtration then washed with de-ionized water and ethanol three times. The final product was vaccum dried at 120 ˚C for 12 hours.
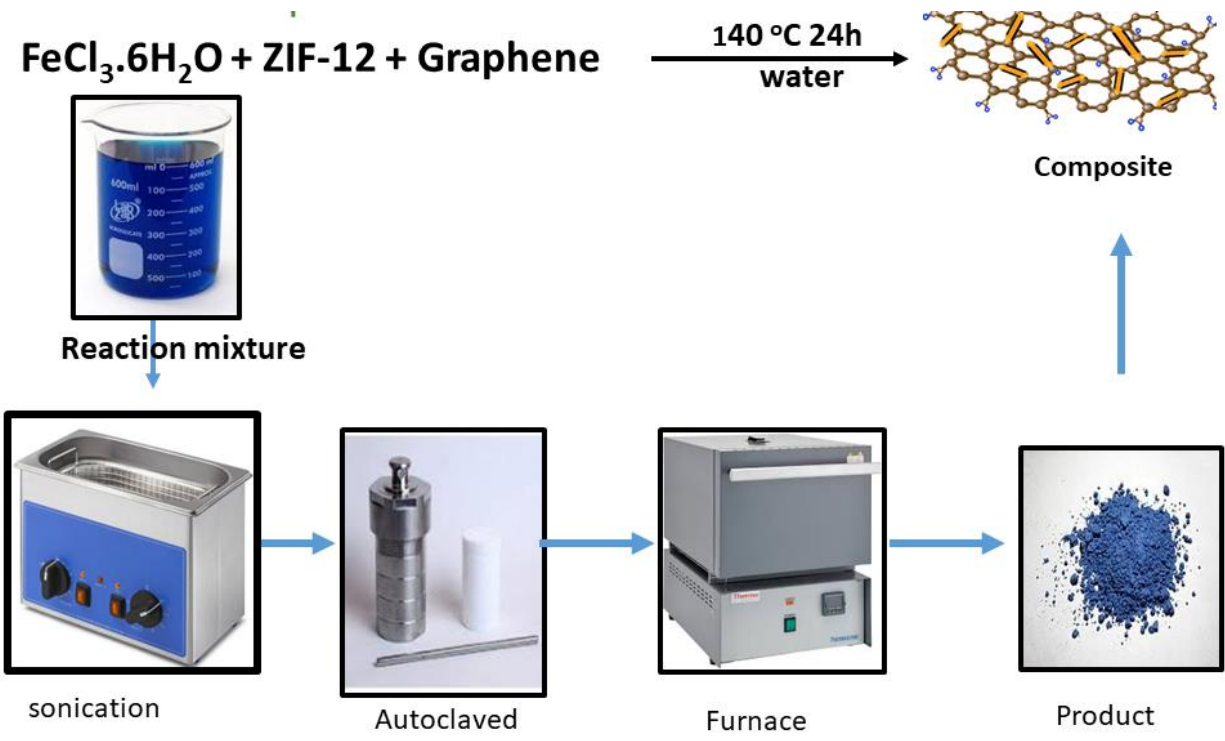
Figure 2.3: Systmatic diagram of synthesis of MOF based composite by hydrothermal method

2.3. Fabrication of electrode:

The FTO was febricated by using drop costing method. The 5 mg of composite was disperse in 1mL of methanol and 20µL of nafion binder than the whole mixture was sonicated for 3 hours to make homogeneous ink. The ink was coated on the surface of the FTO. This coated electrode was dried in oven at 55 ˚C for 12 hours. MOF based coated composite FTO used as working electrode for electrochemical oxygen evolution reaction. The systematic procedure of fabrication of FTO given in the figure (2.4).
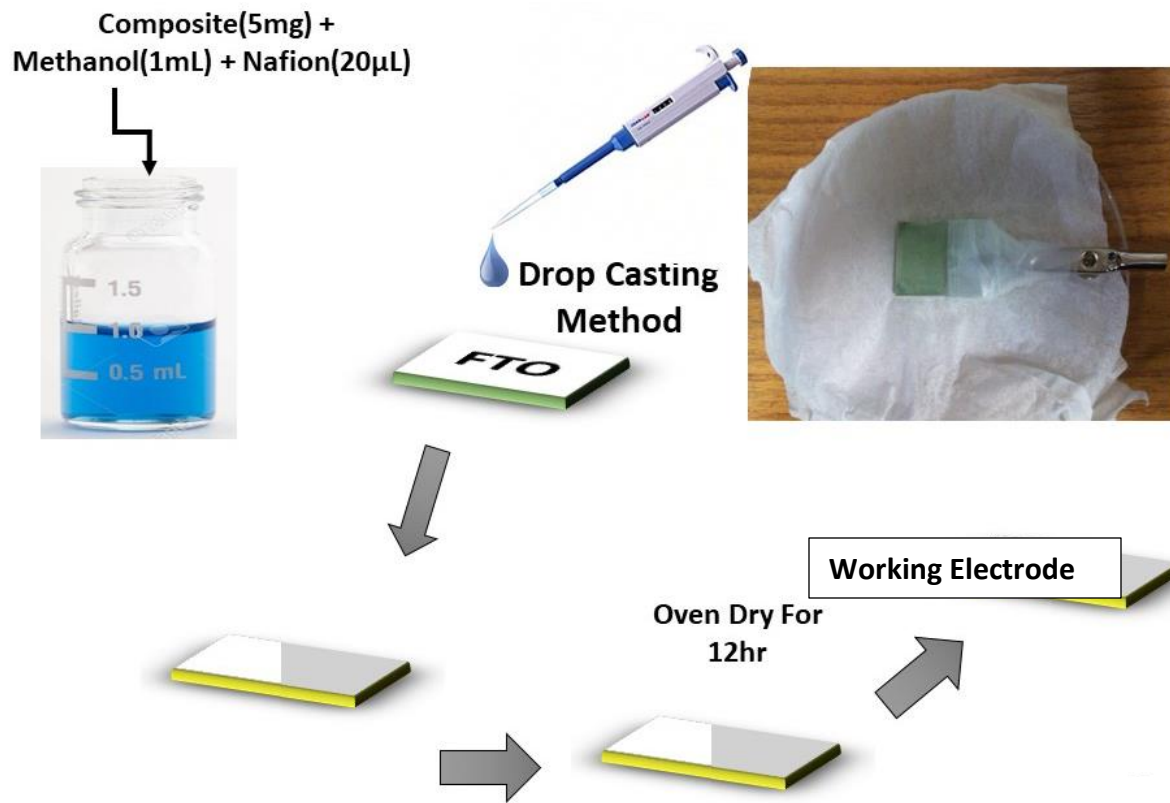
Figure 2.4: Febrication of FTO by drop coasting method to make working electrode

Chapter 3

Theoretical background of the experimental techniques:

This section includes the basic experimental techniques background which I was used in the characterization and electrochemical application. For characterization I used scanning electron microscopy, transmission electron microscopy, x-rays diffraction, thermal gravimetric analysis, elemental analysis and I checked the catalytic activity using techniques chronoamperometry, linear sweep voltammetry and cyclic voltammetry.

3.1. Scanning Electron Microscopy:

The scanning electron microscopy gives the micrographs of morphology of the composite surface. In SEM a beam of high energy electrons is used for the generation of signals having high energy to scan the surface of different material. The signals that originates from the interaction of electron with sample make known information about the sample including morphology, chemical composition and crystalline structure etc.
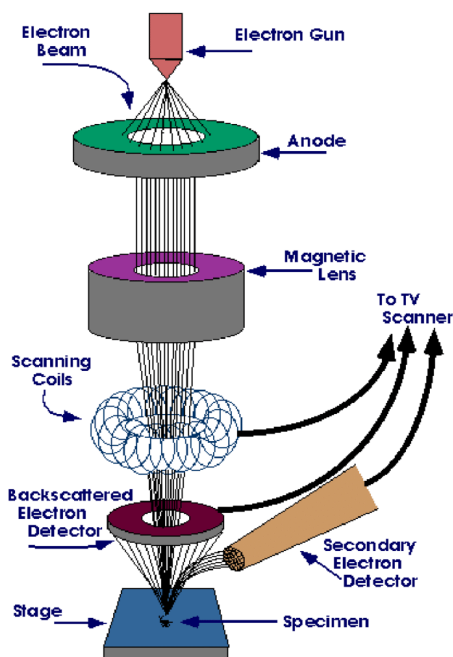
Figure 3.1: Systematic diagram of SEM showing different fundamental components (reproduced from[63])

3.2. Transmission electron Microscopy:

The transmission electron microscopy gives the internal structure image of the material like packing, shape of the particles, crystallinity of the materials, layering of the depositing materials. The story of TEM started when Julius Plucker first observed the electron[64]. He found anew phenomenon in which fluorescent patch was seen opposite to the cathode in the discharge tube. At that time the origin of Cathode rays was known. In 1932 electron lenses were developed and the first idea of electron microscope was proposed to observe the very micro objects[65]. This electron microscope was further modified to look out the internal structures of the objects.

Now a days the TEM is one of most commanding tools to investigate the material on atomic level. Using aberration correction, it is possible to achieve 0.5 A˚ resolution[66]. If the arrangement of individual atomic column in crystal can be visualized, the technique is called resolution TEM (HRTEM). TEM allows one to determine not only morphology and crystal structure of specimens, but also their chemical composition[67].
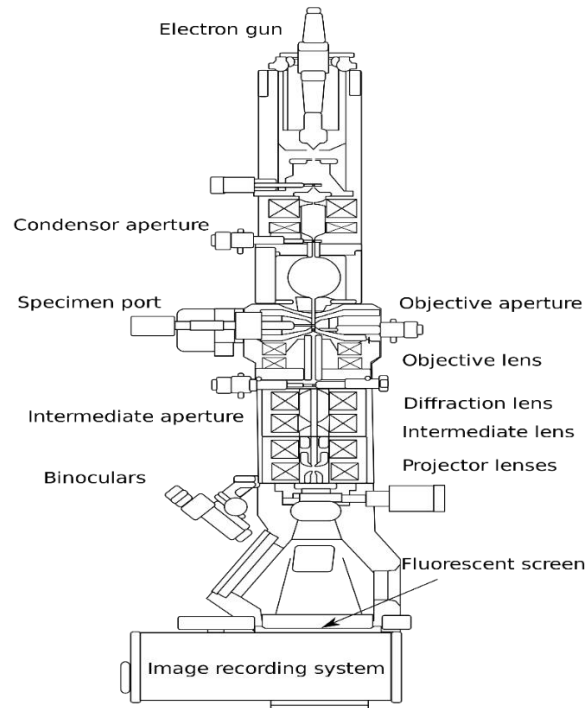

Figure 3.2: Systematic diagram of TEM showing different fundamental components (reproduced from[68])

3.3. X-Rays Diffraction:

XRD used for phase identification of material having the crystalline nature[69]. The basic principle of XRD is based on interaction of X-Rays with electrons of crystalline materials. The interaction of these rays with sample the produces constructive interference when condition satisfy Bragg's equation ($n\lambda=2d\sin\theta$). This law relates different parameters (λ, θ, d) in a crystalline sample[70]. XRD technique is used to determine the particle and crystallinity of the materials.
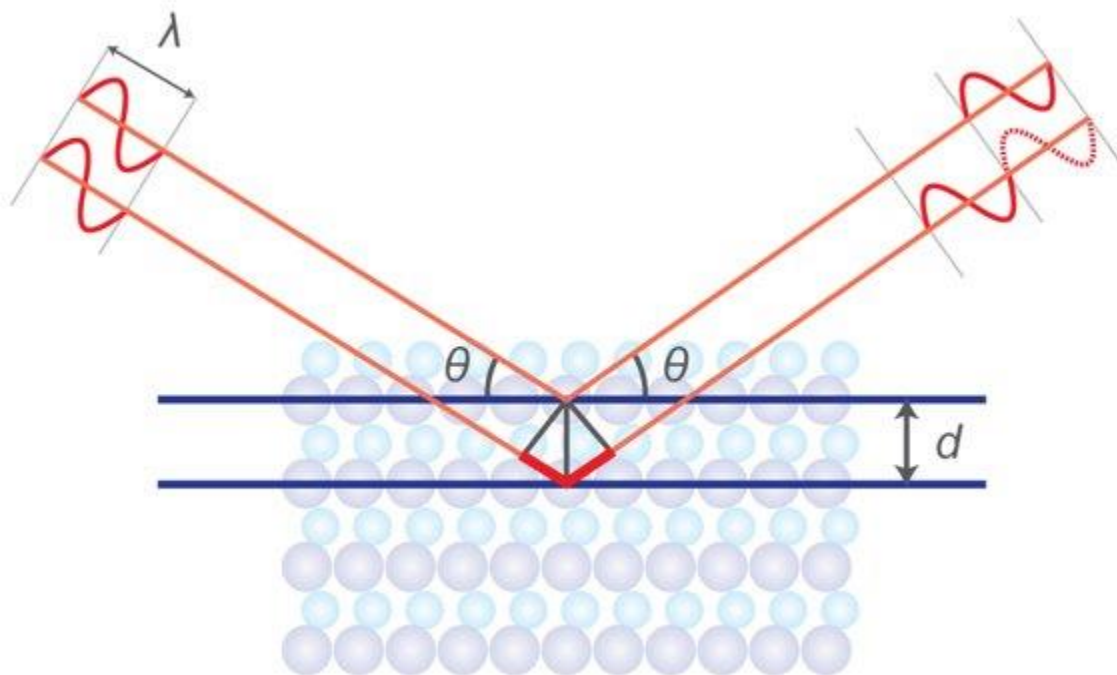
Figure 3.3: Systematic diagram of diffraction of X-Rays from crystal lattice of a crystalline material (reproduced from[71])

3.4. X-Rays Photoelectron Spectroscopy (XPS):

The technique is used to determine the precise composition of the compound, composite, complexes[72]. It also reveals the oxidation state of element more accurately metals. XPS explain the oxidation state energy relation ship between binding energy and oxidation state of the element which is the part compound. Transition metals mostly exist more then one oxidation state so the for the conformation of the oxidation state XPS being performed[73]. The principle of the XPS is the specimen is exposed to X-Rays having the energy $h\upsilon$[74]. The X-Rays mono chromatic photons extract the electrons from the atom present at the surface region. The electrons emitted by the

lower energy rays are called the photon electrons[75]. The systematic diagram is showed in the figure.
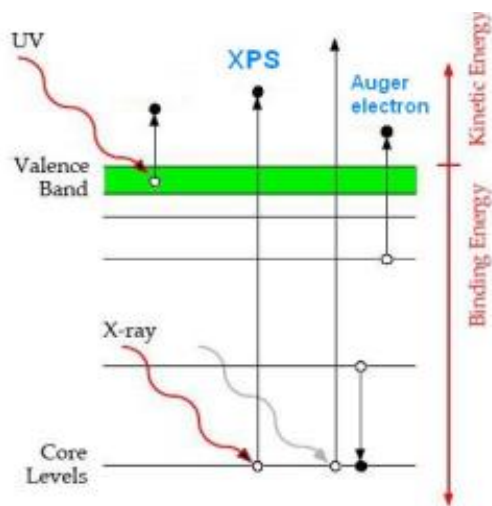
Figure 3.4: Systematic diagram of phenomenon of XPS

3.5. Cyclic Voltammetry (C.V):

CV is electrochemical technique use to check the redox properties of the catalyst, onset potential and current produced in the electrochemical reaction[76]. In the CV the working electrode potential is measured with a specific electrode which is called reference electrode[77]. The purpose of the reference electrode to maintain the constant potential. The graphical representation shown the figure (3.5). in the forward negative scan, the potential start from the high voltage and end at the low voltage.
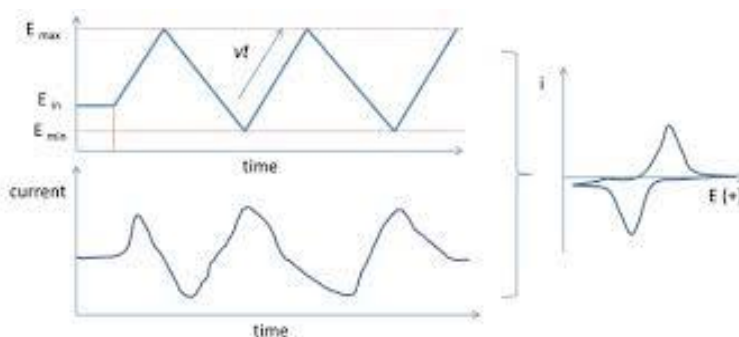
Figure 3.5: Cyclic Voltammogram (reproduced from[78])

Chapter 4

Result and discussion

4.1. Characterization:

The synthesized composite was characterized by using physical as well as chemical techniques for the conformation of the composing material. Synthesized composite was characterized by using following techniques.
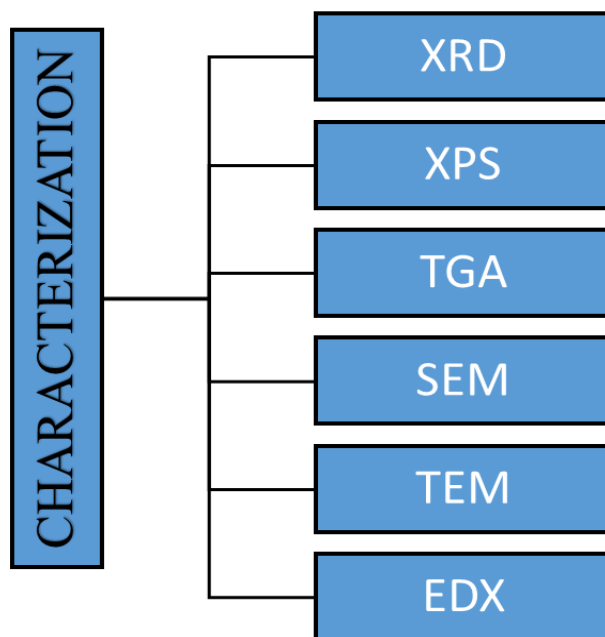
4.1.1. X-Rays Diffraction Spectroscopy:

In order to follow the microstructural evolution of the composite XRD were performed. The XRD pattern ZIF-12 shows the peaks which is shown figure 17. The characteristic peak of ZIF-12 present at position of (12.2˚) and other minor peaks are present at 19, 21.3˚, 22.2˚ and 24.8˚ which are shown in the XRD graph. The XRD pattern of iron oxyhydroxide and graphene composite shows the peaks. The characteristic peak of iron oxyhydroxide is present at 25.5˚. the other minor peaks of iron oxyhydroxide are present from 35.5 ˚ to 55.5˚.

The final composite has all the peaks of iron oxyhydroxide and ZIF-12. The final composite XRD pattern clearly shows that there is a physical interaction between ZIF-12 and iron oxyhydroxide[71].
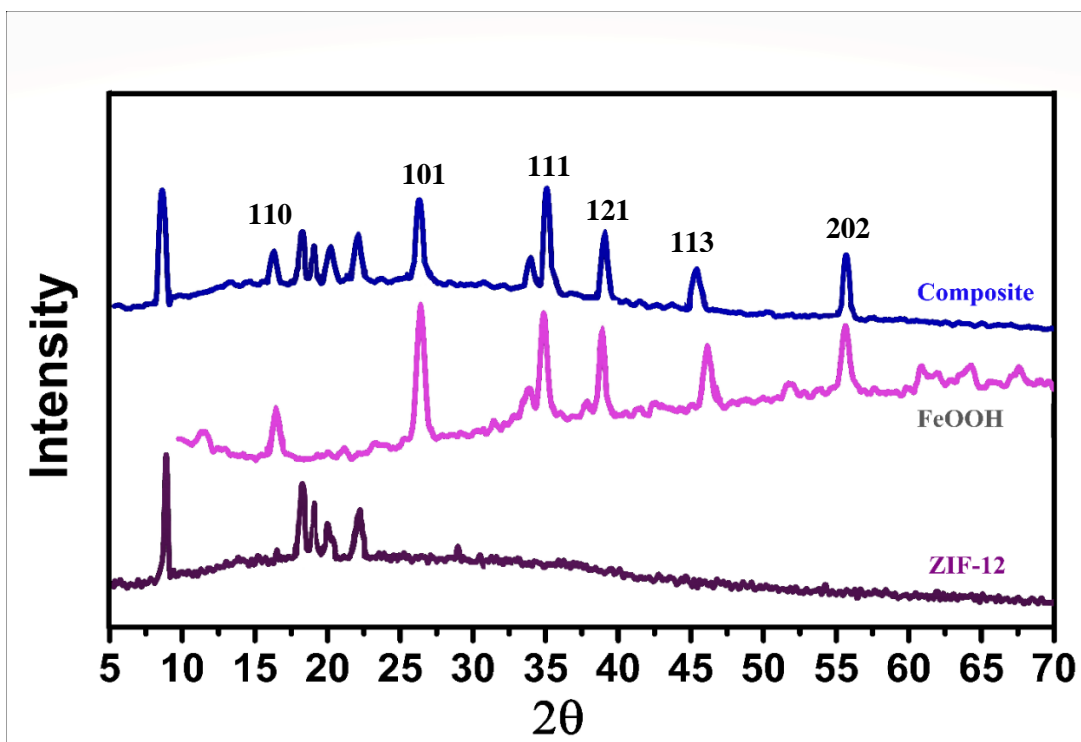
Figure 4.1: XRD Graph shows the pattern of ZIF-12 (blue), iron oxyhydroxide/graphene (pink) and ZIF based composite (green)

4.1.2. Thermal Gravimetric Analysis (TGA):

The thermal gravimetric analysis shows that percentage weight with respect to temperature. The 1st bend shows 7% loss of total mass which includes the mass of water and N,N-Dimethylformamide. The 2nd bend shows the 54% loss of total mass which includes the mass of graphene and benzimidazole ligand. The remaining 39% mass is the mass of the oxides of cobalt and iron which is further elaborate in the given figure (4.2).

The thermogram of the composite shows the stability of the catalyst. The synthesized composite is stable up to 150˚C. After that temperature it decompose into its fragments.
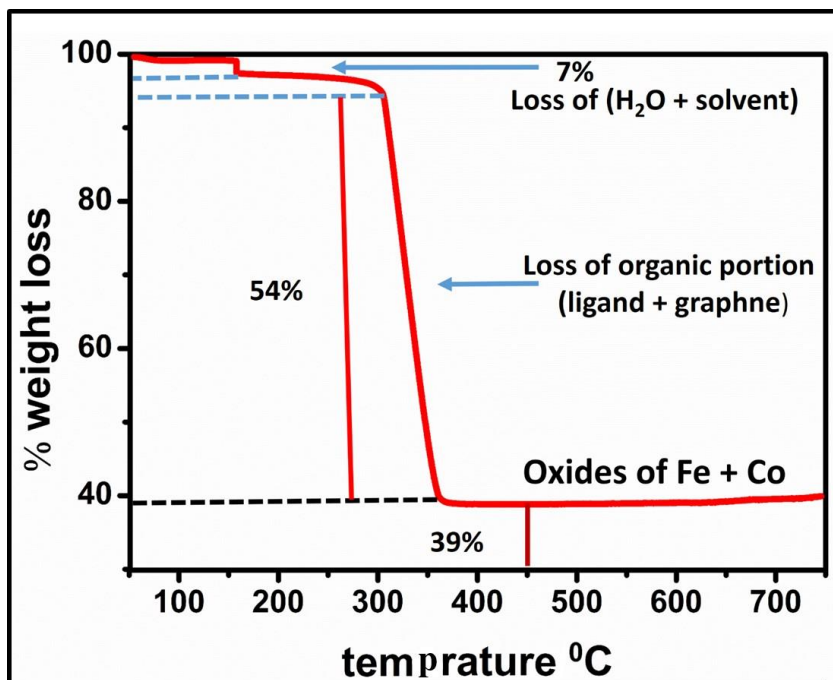
Figure 4.2: Thermogram of composite showing weight loss and stability of remaining oxide up to 750 ˚C

4.1.3. Scanning Electron Microscopy:

The scanning electron microscopic images of composed are shown in the (Fig a, b). it shows the surface morphology of synthesized material. The micrographs show the porous relates to the ZIF-12 and single and multilayer flakes in of graphene are present in the composite.
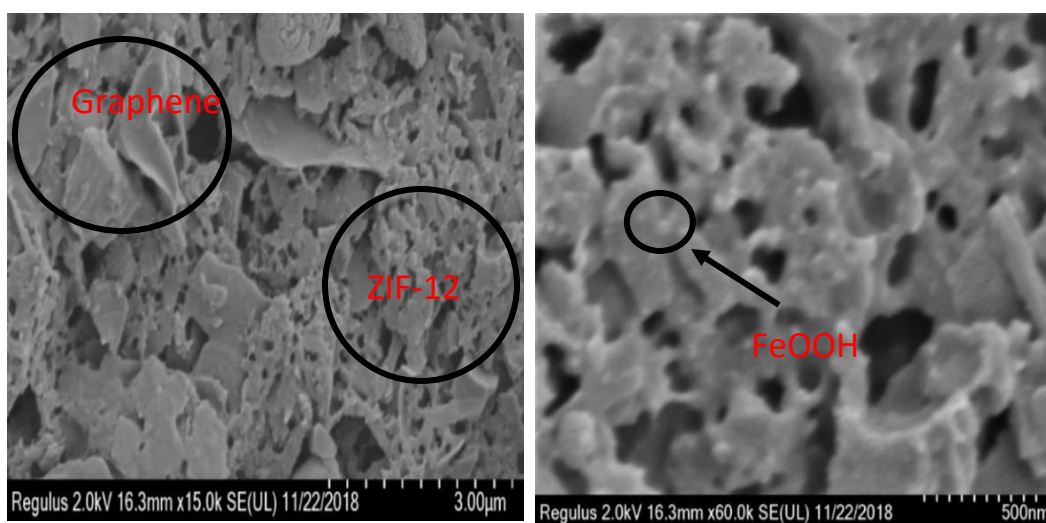
Figure 4.3: SEM Images of Composite showing morphology of electrocatalyst

4.1.4. Transmission Electron Microscopy:

Transmission electron micrograph reveals the internal structure of the composite. It shows the presence of graphene and ZIF-12 in the composite.
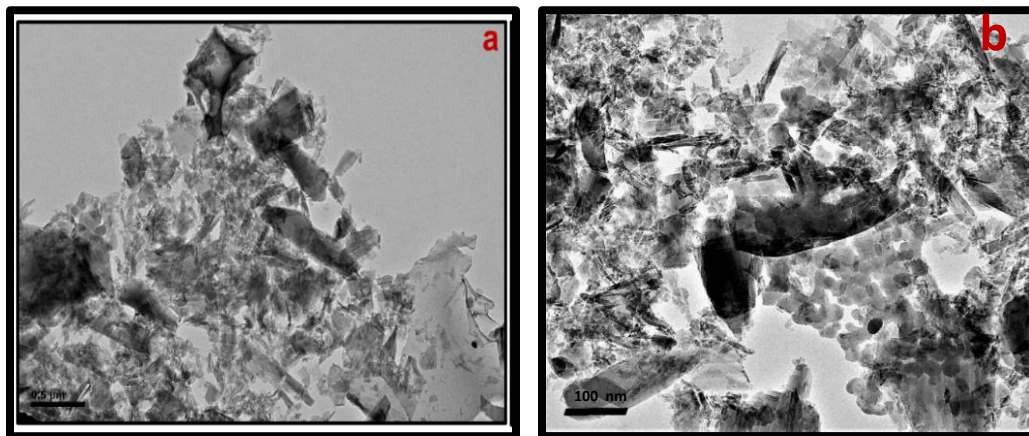
Figure 4.4: TEM Images of Composite showing internal composition of electrocatalyst.

4.1.5. Energy dispersive X-rays spectroscopy:

This technique is used to know the elemental composition of composite. The relative peaks confirm the presence of cobalt, iron, carbon and oxygen in the composite and their percentages.
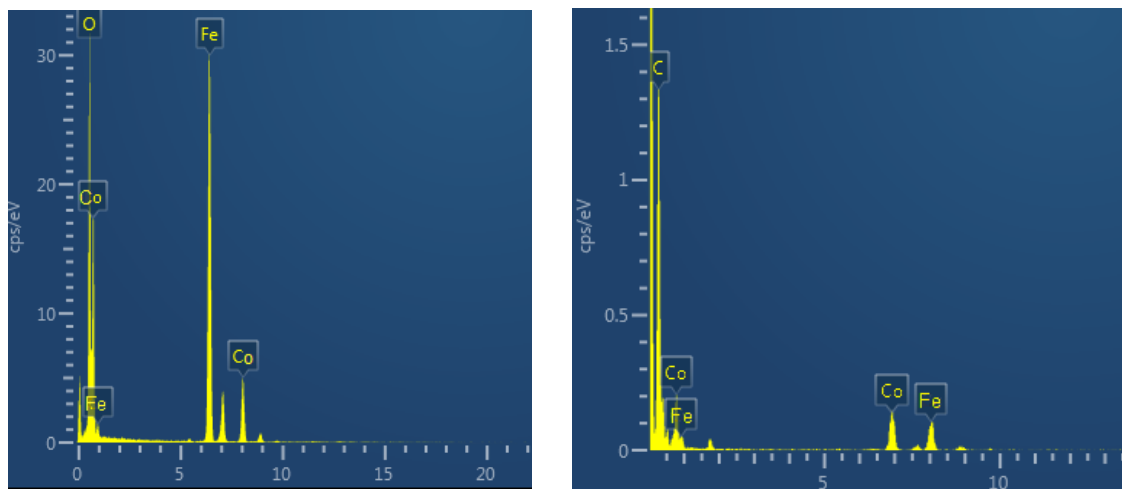
Figure 4.5: EDX Image showing relative peaks of Fe, Co, C and O.

The relative percentages given in the table which confirms the relative intensity of Fe, Co, O and C.

Sr No	Element	Percentage
1	Fe	26
2	Co	23
3	C	33
4	O	18

Table 4: Relative percentages of different Element present in composite

4.1.6. X-Ray Photoelectron Spectroscopy:

The XPS shows the relationship between binding energy value and oxidation state of the element. XPS spectra of iron, carbon, cobalt and oxygen shown in the figure (4.6). The XPS spectra of cobalt shows peaks range from 780 eV to 805 eV. The major peak in the cobalt spectrum at 781 eV for Co2p3/2. The satellite peak for Co2p3/2 is present at 786 eV. The major peak for Co2p1/2 is present at the 796 eV and the satellite peak for Co2p1/2 is present at the 803 eV. The intensities of the satellite are lower. The binding energy values shows that cobalt is present in the 2+ oxidation state and which is component of the ZIF-12. The binding energy value for cobalt in ZIF-12 almost matches with reported ZIF-12 which confirms that synthesized composite contains MOF. The XPS spectrum exactly matches with reported ZIF-12 XPS.
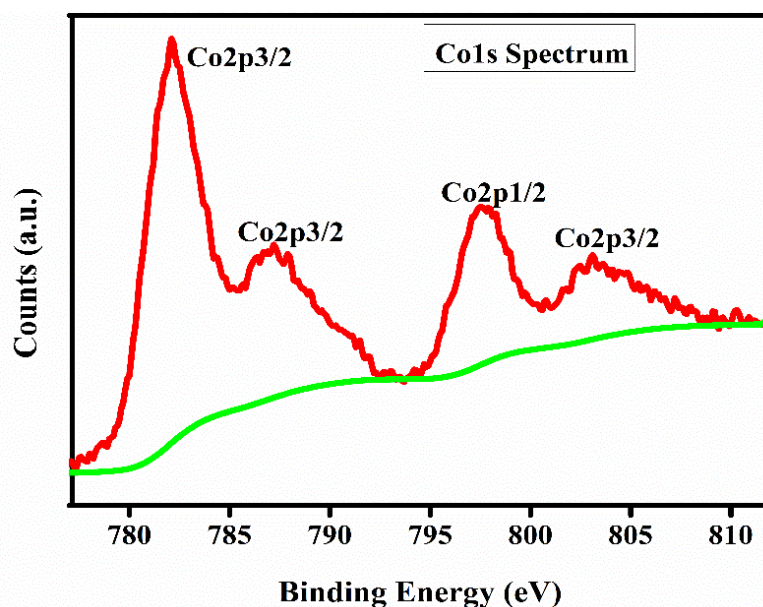
Figure 4.6: XPS spectrum of cobalt for MOF

The XPS spectrum of iron shows peaks range from 708 eV to 735eV as given figure (4.7). The major peak in the cobalt spectrum at 711eV for Fe2p3/2. The satellite peak for Fe2p3/2 is present at715 eV. The major peak for Fe2p1/2 is present at the 727eV and the satellite peak for Fe2p1/2 is present at the 733eV.
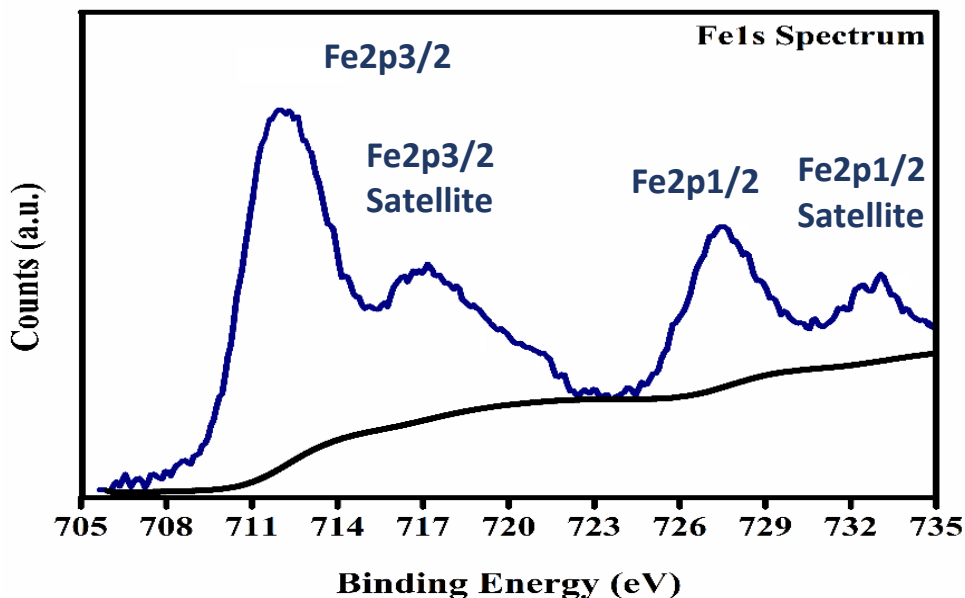
Figure 4.7: XPS spectrum of iron for FeOOH

The intensities of the satellite are lower. The binding energy values shows that iron is present in the 3+ oxidation state and which is component of the iron oxyhydroxide.
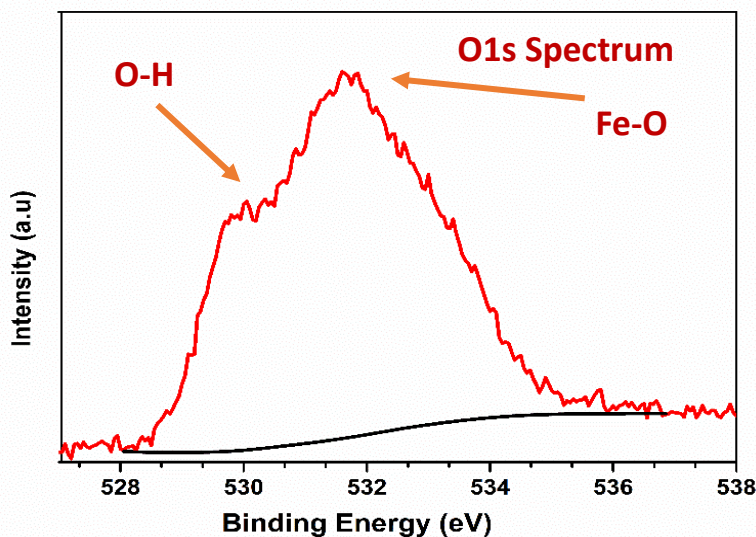
Figure 4.8: Oxygen XPS spectrum for FeOOH.

The XPS spectrum of oxygen shows the peaks of Fe-O and O-H at the 529.5 eV and 532 eV respectively shown in figure (4.8). The intensity of O-H lower than the Fe-O.

In order to study the nature of carbon in composite C1s XPS is a useful tool. For graphene peaks centred at 284-285 eV are mostly assigned to sp^2 species[79]. The carbon is constituent of both graphene and imidazole in both, carbons is sp^2 hybridized. The binding energy values are exactly matched with reported XPS spectrum of carbon.
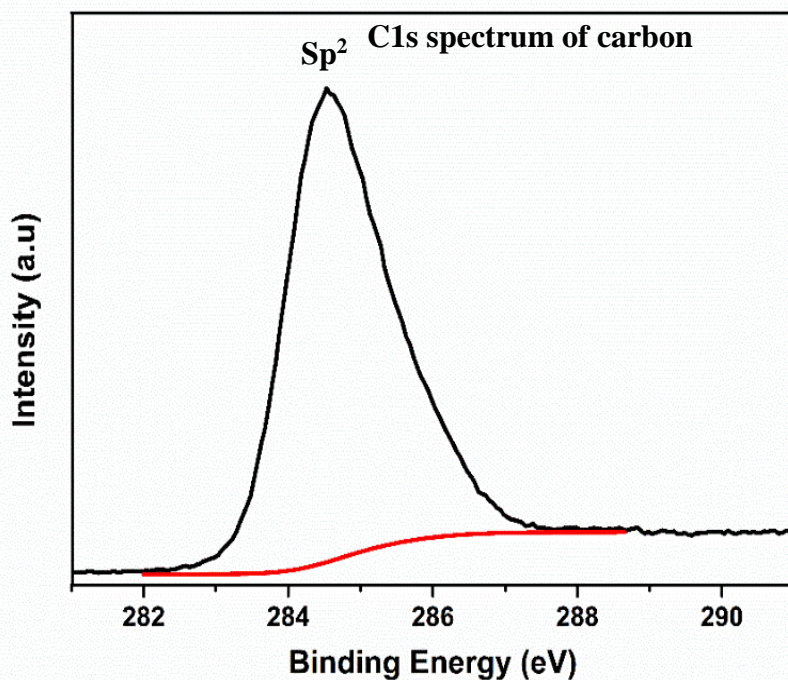
Figure 4.9: Carbon XPS spectrum

4.2. Electrochemical studies for Water Oxidation:

The electrocatalytic activity was performed by using electrochemical cell which was connected with potentiate (Gamry E-500). In the studies coated FTO was used working electrode, Ag/AgCl as reference electrode and Pt wire as counter electrode. 0.5 M KOH solution was used as electrolyte. The systematic diagram of electrochemical cell is shown in the figure (4.11).
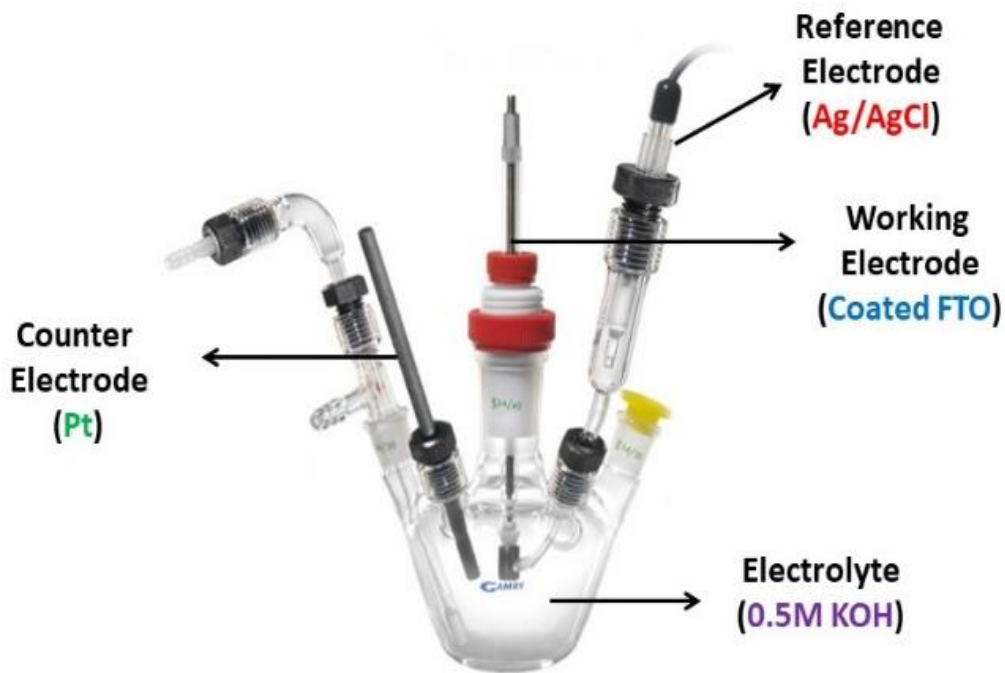
Figure 4.10: Electrochemical Cell used to check the catalytic activity of synthesized composite.

Overpotential:

The potential required to produce anodic or cathodic current at specific voltage in an electrochemical reaction. Overpotential is always greater than thermodynamic potential. The appropriate parameter to check the catalytic activity of electrocatalyst is overpotential. For a best catalyst the value of overpotential should be minimum.

4.2.1. Linear sweep voltammetry for oxidation of water by FeOOH/Graphene:

Linear sweep voltametric experiments for water oxidation were performed by using 0.5M KOH solution at the scan rate 100 V/s. its current increase as a function of applied voltage. The current density and onset potential were change with change the concentration of iron oxyhydroxide and graphene. The maximum results obtained when the ratio between iron oxyhydroxide and graphene was 1:1. Results of iron oxyhydroxide and graphene are shown in the figure (4.11). The overpotential of synthesized composite calculated by using Nernst equation.

$$\text{Over potential} = [E_{Ag/AgCl} + 0.0591(pH) + 0.1976] - 1.23$$

The pH value for electro water oxidation in our studies is 12 for 0.5 M KOH solution. The value 1.23 is thermodynamic potential for OER[47].
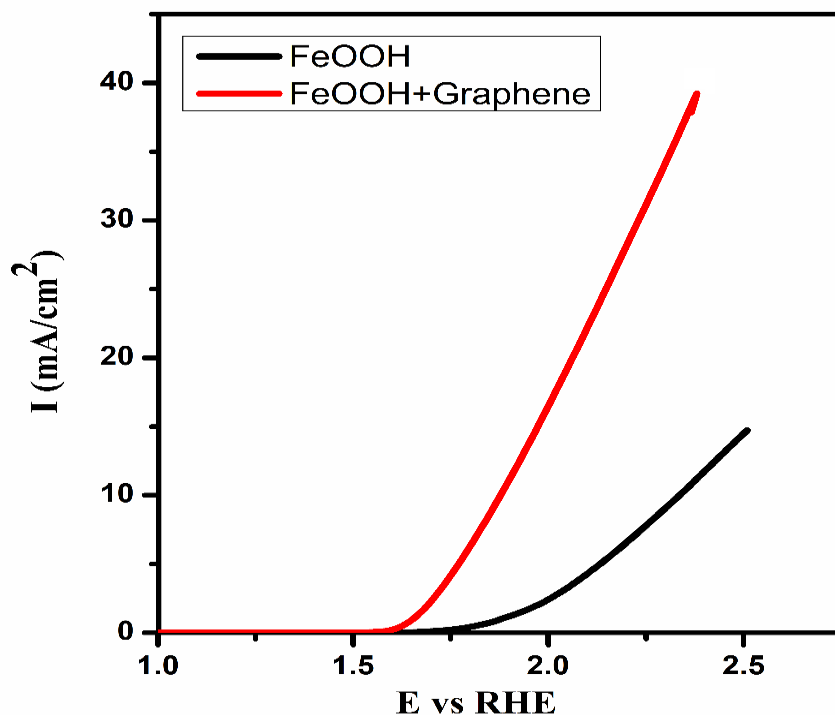
Figure 4.11: Voltammogram FeOOH and FeOOH/Graphene showing activity of electrocatalytic in 0.5 M KOH solution as electrolyte having pH 12.

4.2.2. Linear sweep voltammetry for oxidation of water by MOF based FeOOH/Graphene composite:

The electrocatalytic activity for water oxidation was performed by using linear sweep voltammetry. The catalytic activity was calculated by measuring current density, overpotential, tafel slope and turn over frequency. The voltammogram of catalyst shows the current density is 101 mA/cm^2 and to attain overpotential is 291 mV the current density of 10 mA/cm^2. The overpotential shown by the ZIF-12 is 530 mV for current density 10 mA/cm^2 and 480 mV overpotential was shown by iron oxyhydroxide/graphene composite for same current density as composite and ZIF-12. The linear sweep voltammogram shown in the figure (4.12).
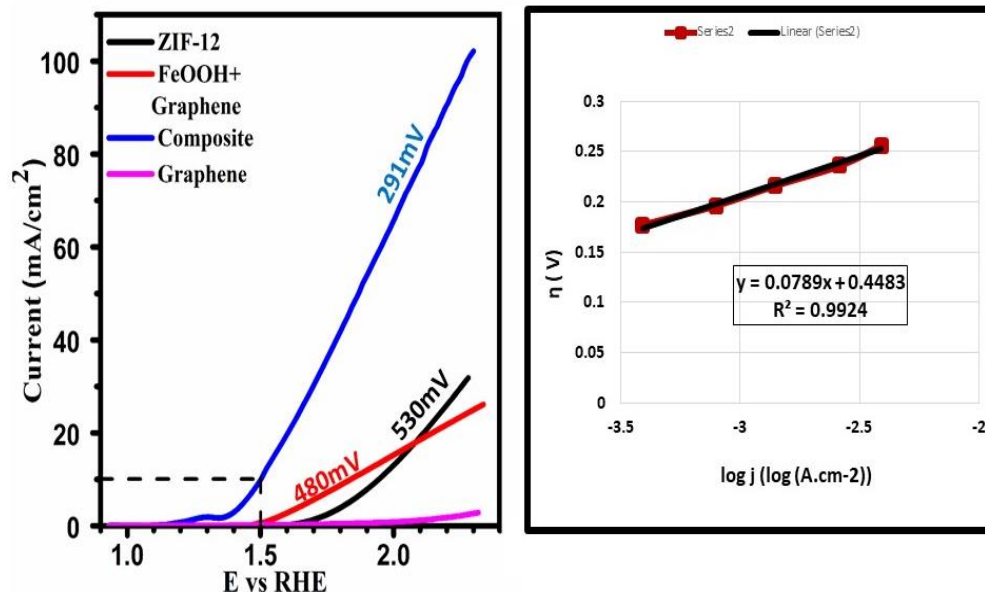
Figure 4.12: Voltammogram and tafel plot of synthesized composite in 0.5 M KOH solution having pH 12.

4.2.2.1. Catalytic activity with varying concentration:

The catalytic activity was checked by varying the concentration of iron oxyhydroxide and ZIF-12. When the concentration of iron oxyhydroxide and ZIF-12 was 1:1 the composite showed maximum current density and minimum overpotential.
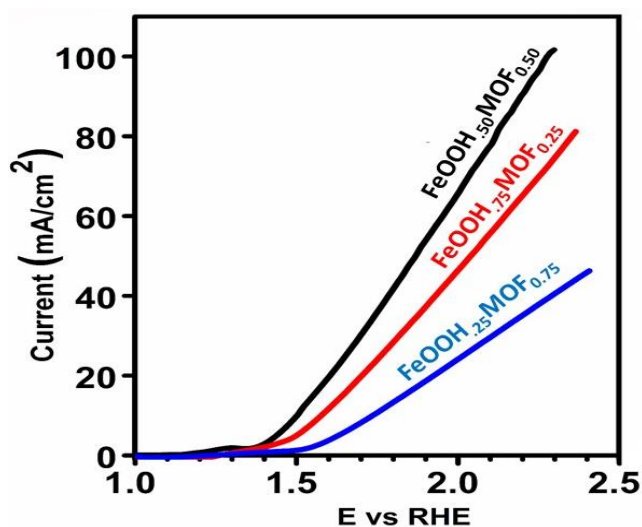
Figure 4.13: Voltammogram with varying concentration of iron oxyhydroxide and MOF in composite showing different electrocatalytic activity.

Beyond this concentration with changing the concentration of ZIF-12 and iron oxyhydroxide the onset potential moves towards high anodic region and the current density decreased as shown in the figure (4.13). The aim of these studies was to check the major catalytic sites in the composite which was iron oxyhydroxide. With increase the concentration of iron oxyhydroxide, catalytic activity of composite increased.

4.2.3. Tafel slope:

The 2nd parameter to check the catalytic efficiency of composite is Tafel slope. For the best catalytic activity, the Tafel slope should be minimum. The Tafel slope value for ZIF-12, iron oxyhydroxide/graphene and composite are 172, 109 and 78mV/dec respectively. The final composite shows lower value of slop as compare to ZIF-12 and iron oxyhydroxide/graphene. The value of Tafel slopes tells the number of transfers of electron in the reaction[80].
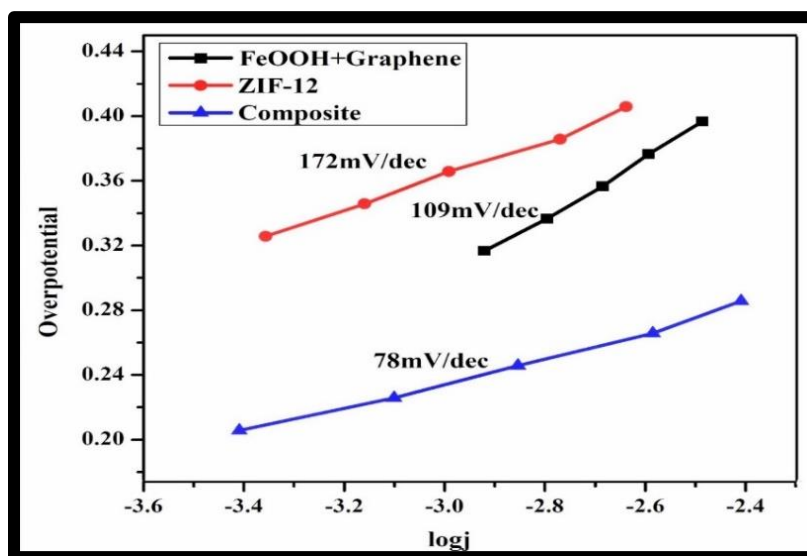
Figure 4.14: Tafel plot of MOF based composite at current of 10 mA in 0.5 M KOH solution.

The Tafel slope for synthesized composite shows that, mechanism of reaction 3rd electron transfer is rate determining step.

4.2.4. Turn Over Frequency (TOF):

Another parameter to check the catalytic activity of the electrocatalyst is measure the turn over frequency. Turn over frequency can be calculated by using the formula

TOF= J×A/4F×m

J = current density for specific overpotential

A = area of electrode

F = faraday constant

m = moles of active centre

The TOF was calculated at different overpotential and current. The composite graph shown in the table 4.

Table 4: TOF value at different overpotential

Sr No	Current Density (mA/cm^2)	Over potential (mV)	TOF(s^{-1})
1	1	266	0.0011
2	10	291	0.01031
3	20	314	0.0301
4	30	326	0.0467
5	40	338	0.0593
6	50	346	0.0720
7	101	369	0.1012

Activity table of FeOOH, ZIF-12 and graphene based electrocatalyst is shown in the table

Sr No	Catalyst	Over potential (mV)	Tafel slope (mV/dec)	Current density(mA)	Electrolyte
1	FeOOH	630	130	20	0.5 M KOH

2	FeOOH$_{0.75}$:Graphene$_{0.25}$	567	123	22	0.5 M KOH
3	FeOOH$_{0.5}$:Graphene$_{0.5}$	480	109	36	0.5 M KOH
4	ZIF-12	530	172	26	0.5 M KOH
5	FeOOH$_{0.75}$:ZIF-12$_{0.25}$/graphene	350	-	81	0.5 M KOH
6	FeOOH$_{0.25}$:ZIF-12$_{0.75}$/Graphene	590	-	46	0.5 M KOH
7	**FeOOH$_{0.5}$:ZIF-12$_{0.5}$/graphene**	**291**	**78**	**101**	**0.5 M KOH**

4.2.5. Stability of Electrocatalyst:

The stability of electrocatalyst was checked by using following techniques.

- Chronoamperometry.
- Cyclicvoltametry.
- X-rays photoelectron spectroscopy.

5.2.5.1. Through Chronoamperometry (CA):

The catalytic stability of catalyst was checked by performing the chronoamperometry (CA) at 1.00 volts against Ag/AgCl reference electrode for 9h. There was no major fluctuation in the peak which showed that synthesized composite was stable at high current density 47 mA/cm^2. The CA graph is shown in the figure (4.15). The synthesized electrocatalyst was stable up to 9 hours in 0.5 M KOH solution at current density of 47mA. The catalytic activity remained same after performing 9 hours chronoamperometry.
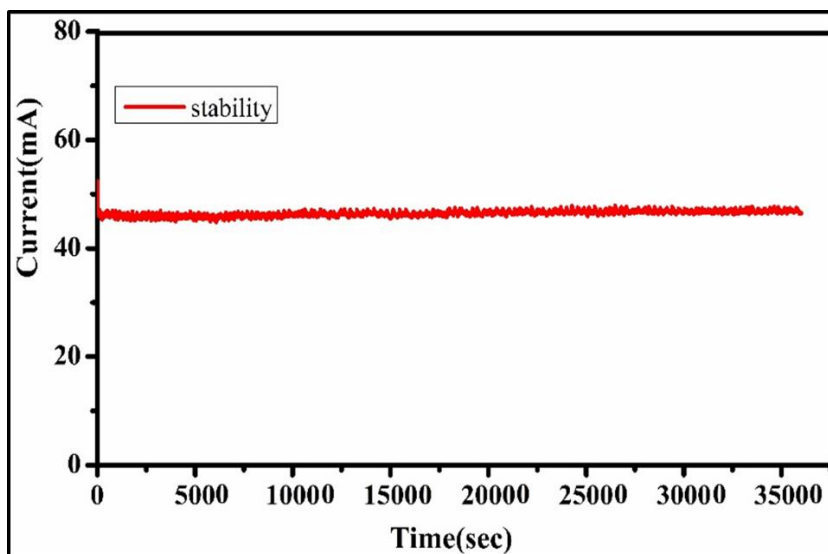
Figure 4.15: Chronoamperometry spectrum at 47 mA current in 0.5 M KOH solution

4.2.5.2. Stability through cyclic voltammetry:

The stability of catalyst was checked by performing cyclic voltammetry before and after the oxygen evolution reaction. There was no major change occurred in the peak shape and current density shown in the figure (4.16).
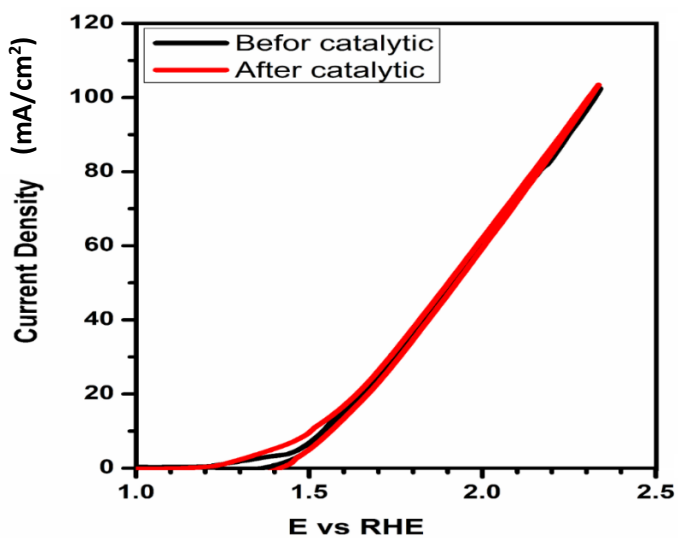
Figure 4.16: Cyclic Voltammogram before and after catalytic activity

So, the synthesized catalyst was stable before and after the catalytic activity.

4.2.5.3. Stability through XPS:

The stability of was also checked by performing the XPS before and after the catalytic activity of electrocatalyst. The peak positions remained same before and after electrocatalytic water oxidation activity shown in the figure (4.17).
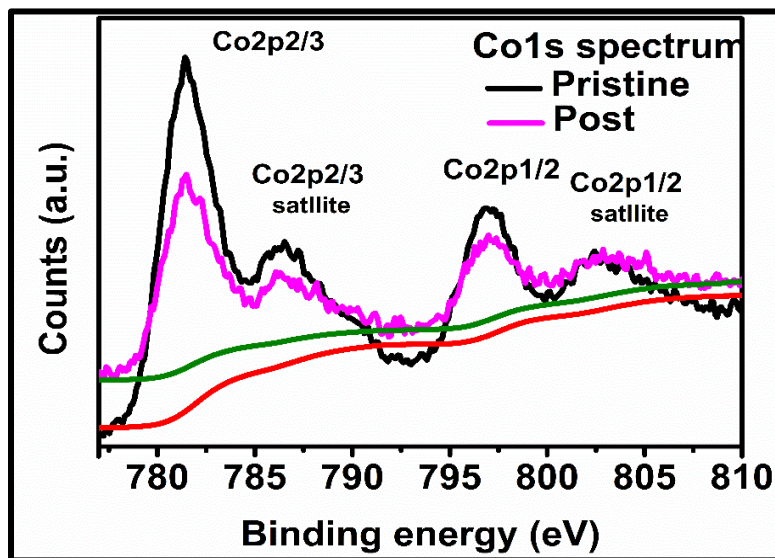
Figure 4.17: XPS spectrum of cobalt shoeing stability of catalyst before and after catalytic activity

Conclusion:

A novel water splitting electrocatalyst of FeOOH-based composite (FeOOH$_{0.5}$:ZIF-12$_{0.5}$/Graphene) was synthesized using facile and low-cost method compared to traditional precious noble-metal-based electrocatalyst such as RuO$_2$ and IrO$_2$. The present studies show the results of iron oxyhydroxide deposited on ZIF-12 and graphene composite catalytic performance for electrocatalytic water oxidation. The final composite (FeOOH$_{0.5}$:ZIF-12$_{0.5}$/Graphene) was characterized by XRD, TEM, TGA and XPS. The composite (FeOOH$_{0.5}$:ZIF-12$_{0.5}$/Graphene) was found to have excellent performance for accelerating OER with a very low overpotential and high current density. The linear sweep voltammetric results revealed that a current density of 10 mA/cm^2 demanded overpotential of just 291 mV in 0.5M KOH solution thus suggesting high OER efficiency of modified iron oxyhydroxide. Also checked the effect of change of concentration of iron oxyhydroxide and ZIF-12 on electrocatalytic activity of composite. Furthermore, the robustness of this MOF based electrocatalyst during water oxidation was evidenced by the generation and gushing out of oxygen bubbles at the surface of modified FTO. All of above advantages of hydrothermal synthesized OER electrocatalyst (FeOOH$_{0.5}$:ZIF-12$_{0.5}$/Graphene) indicate that iron, cobalt has great potential to contribute in ensuring carbon-based energy economy in the further advanced devices for clean energy production.

References:

1. Simmons, M., Twilight in the Desert. Hoboken. NJ: John Wiley & Sons: 2005, 52-98.

2. Tertzakian, P., A thousand barrels a second: The coming oil break point and the challenges facing an energy dependent world. **2007**, 6 (18), 22-36.

3. Armaroli, N.; Balzani, V., The future of energy supply: challenges and opportunities. *Angew. Chem.* **2007,** *46* (1-2), 52-66.

4. Wackernagel, M.; Schulz, N. B.; Deumling, D.; Linares, A. C.; Jenkins, M.; Kapos, V.; Monfreda, C.; Loh, J.; Myers, N.; Norgaard, R., Tracking the ecological overshoot of the human economy. *Proc. Natl. Acad. Sci. U.S.A.* **2002,** *99* (14), 9266-9271.

5. Rand, D. A. J.; Dell, R. M., *Hydrogen energy: challenges and prospects*. Roy. Soc. Chem. 2007.

6. Majeed, I.; Nadeem, M. A.; Al-Oufi, M.; Nadeem, M. A.; Waterhouse, G.; Badshah, A.; Metson, J.; Idriss, H., On the role of metal particle size and surface coverage for photo-catalytic hydrogen production: A case study of the Au/CdS system. *Appl. Catal. Environ.* **2016,** *182*, 266-276.

7. Reichert, R.; Jusys, Z.; Behm, R. J. r., Au/TiO2 photo (electro) catalysis: the role of the Au cocatalyst in photoelectrochemical water splitting and photocatalytic H_2 evolution. *J. Phys. Chem. C.* **2015,** *119* (44), 24750-24759.

8. Ally, J.; Pryor, T., Life-cycle assessment of diesel, natural gas and hydrogen fuel cell bus transportation systems. *Journal of Power Sources* **2007,** *170* (2), 401-411.

9. Cheng, W.; Zhao, X.; Su, H.; Tang, F.; Che, W.; Zhang, H.; Liu, Q., Lattice-strained metal–organic-framework arrays for bifunctional oxygen electrocatalysis. *Nat. Ener.* **2019**, 1.

10. Lipkowski, J.; Ross, P. N., *Electro catal.* 1998; Vol. 3.

11. Seshadri, G.; Lin, C.; Bocarsly, A. B., A new homogeneous electrocatalyst for the reduction of carbon dioxide to methanol at low overpotential. *J. Electro. Chem.* **1994,** *372* (1-2), 145-150.

12. Wang, D.; Groves, J. T., Efficient water oxidation catalyzed by homogeneous cationic cobalt porphyrins with critical roles for the buffer base. *Proc. Natl. Acad. Sci. U.S.A.***2013**, 15-83.

13. Rossmeisl, J.; Qu, Z.-W.; Zhu, H.; Kroes, G.-J.; Nørskov, J. K., Electrolysis of water on oxide surfaces. *J. Electro. Chem.* **2007,** *607* (1-2), 83-89.

14.   Suen, N.-T.; Hung, S.-F.; Quan, Q.; Zhang, N.; Xu, Y.-J.; Chen, H. M., Electrocatalysis for the oxygen evolution reaction: recent development and future perspectives. *Chem. Rev.* **2017,** *46* (2), 337-365.

15.   (a) Marshall, A. T.; Sunde, S.; Tsypkin, M.; Tunold, R., Performance of a PEM water electrolysis cell using IrxRuyTazO2 electrocatalysts for the oxygen evolution electrode. *Int. J. Hydrog. Energy.* **2007,** *32* (13), 2320-2324; (b) De Levie, R., The electrolysis of water. *J. Electro. Chem.* **1999,** *476* (1), 92-93.

16.   Delgado, D.; Hefter, G.; Minakshi, M., Hydrogen generation. In *Alter. energ.* 2013; pp 141-161.

17.   (a) Appleby, A.; Crepy, G.; Jacquelin, J., High efficiency water electrolysis in alkaline solution. *Int. J. Hydrog. Energy* **1978,** *3* (1), 21-37; (b) Parrondo, J.; George, M.; Capuano, C.; Ayers, K. E.; Ramani, V., Pyrochlore electrocatalysts for efficient alkaline water electrolysis. *J. Mater. Chem A.* **2015,** *3* (20), 10819-10828.

18.   Fang, Y.-H.; Liu, Z.-P., Mechanism and tafel lines of electro-oxidation of water to oxygen on RuO2 (110). *J. Am. Chem. Soci.* **2010,** *132* (51), 18214-18222.

19.   (a) Grzelczak, M.; Zhang, J.; Pfrommer, J.; Hartmann, J. r.; Driess, M.; Antonietti, M.; Wang, X., Electro-and photochemical water oxidation on ligand-free Co3O4 nanoparticles with tunable sizes. *ACS Catal.* **2013,** *3* (3), 383-388; (b) Li, G.; Pickup, P. G., The promoting effect of Pb on carbon supported Pt and Pt/Ru catalysts for electro-oxidation of ethanol. *Electrochim. Acta* **2006,** *52* (3), 1033-1037.

20.   Tilly, G.; Sage, W., The interaction of particle and material behaviour in erosion processes. *Wear* **1970,** *16* (6), 447-465.

21.   Chowdhury, D. R.; Spiccia, L.; Amritphale, S.; Paul, A.; Singh, A., A robust iron oxyhydroxide water oxidation catalyst operating under near neutral and alkaline conditions. *J. Mater. Chem A.* **2016,** *4* (10), 3655-3660.

22.   (a) Binninger, T.; Mohamed, R.; Waltar, K.; Fabbri, E.; Levecque, P.; Kötz, R.; Schmidt, T. J., Thermodynamic explanation of the universal correlation between oxygen evolution activity and corrosion of oxide catalysts. *Sci. rep.* **2015,** *5*, 12167; (b) Izgorodin, A.; Winther-Jensen, O.; MacFarlane, D. R., On the stability of water oxidation catalysts: challenges and prospects. *Aust. J. Chem.* **2012,** *65* (6), 638-642.

23.   Patcharavorachot, Y.; Arpornwichanop, A.; Chuachuensuk, A., Electrochemical study of a planar solid oxide fuel cell: Role of support structures. *J. Power Sources* **2008,** *177* (2), 254-261.

24.   Lahav, N.; Chang, S., The possible role of solid surface area in condensation reactions during chemical evolution: reevaluation. *J. Molecule. Evo.* **1976,** *8* (4), 357-380.

25.   (a) Collins, A.; Frost, J. C.; Price, P. J., Method for preparing a catalyst. Google Patents: 1990; (b) Merzougui, B.; Hachimi, A.; Akinpelu, A.; Bukola, S.; Shao, M., A Pt-free catalyst for oxygen reduction reaction based on Fe–N multiwalled carbon nanotube composites. *Electrochim. Acta.* **2013,** *107*, 126-132.

26.   Austin, B. W.; George, H. R., Process for preparing catalyst support and product thereof. Google Patents: 1967.

27.   Schwickardi, M.; Johann, T.; Schmidt, W.; Schüth, F., High-surface-area oxides obtained by an activated carbon route. *Chem. Mater.* **2002,** *14* (9), 3913-3919.

28.   Hameed, B.; Din, A. M.; Ahmad, A., Adsorption of methylene blue onto bamboo-based activated carbon: kinetics and equilibrium studies. *J. Hazard Mater.* **2007,** *141* (3), 819-825.

29.   Gamby, J.; Taberna, P.; Simon, P.; Fauvarque, J.; Chesneau, M., Studies and characterisations of various activated carbons used for carbon/carbon supercapacitors. *J. power sources* **2001,** *101* (1), 109-116.

30.   Siriwardane, R. V.; Shen, M.-S.; Fisher, E. P.; Poston, J. A., Adsorption of CO2 on molecular sieves and activated carbon. *Energy & Fuels* **2001,** *15* (2), 279-284.

31.   Inagaki, M.; Iwashita, N.; Kouno, E., Potential change with intercalation of sulfuric acid into graphite by chemical oxidation. *Carbon* **1990,** *28* (1), 49-55.

32.   Mahto, T. K.; Jain, R.; Chandra, S.; Roy, D.; Mahto, V.; Sahu, S. K., Single step synthesis of sulfonic group bearing graphene oxide: a promising carbo-nano material for biodiesel production. *J. Environ. Chem. Eng.* **2016,** *4* (3), 2933-2940.

33.   Hwang, J.; Kim, M.; Campbell, D.; Alsalman, H. A.; Kwak, J. Y.; Shivaraman, S.; Woll, A. R.; Singh, A. K.; Hennig, R. G.; Gorantla, S., van der Waals epitaxial growth of graphene on sapphire by chemical vapor deposition without a metal catalyst. *ACS Nano.* **2012,** *7* (1), 385-395.

34.   Dreyer, D. R.; Jia, H. P.; Bielawski, C. W., Graphene oxide: a convenient carbocatalyst for facilitating oxidation and hydration reactions. *Angew. Chem.* **2010,** *122* (38), 6965-6968.

35.   Navalon, S.; Dhakshinamoorthy, A.; Alvaro, M.; Garcia, H., Carbocatalysis by graphene-based materials. *Chem rev.* **2014,** *114* (12), 6179-6212.

36.   Huang, C.; Li, C.; Shi, G., Graphene based catalysts. *Energy. Environ. Sci.* **2012,** *5* (10), 8848-8868.

37.   Choi, C. H.; Chung, M. W.; Kwon, H. C.; Park, S. H.; Woo, S. I., B, N-and P, N-doped graphene as highly active catalysts for oxygen reduction reactions in acidic media. *J. Mater Chem. A.* **2013,** *1* (11), 3694-3699.

38.   Yang, H.; Jiang, J.; Zhou, W.; Lai, L.; Xi, L.; Lam, Y. M.; Shen, Z.; Khezri, B.; Yu, T., Influences of graphene oxide support on the electrochemical performances of graphene oxide-MnO 2 nanocomposites. *Nano. Lett.* **2011,** *6* (1), 531.

39.   Zhang, N.; Zhang, Y.; Xu, Y.-J., Recent progress on graphene-based photocatalysts: current status and future perspectives. *Nanoscale* **2012,** *4* (19), 5792-5813.

40.   Lightcap, I. V.; Kosel, T. H.; Kamat, P. V., Anchoring semiconductor and metal nanoparticles on a two-dimensional catalyst mat. Storing and shuttling electrons with reduced graphene oxide. *Nano. Lett.* **2010,** *10* (2), 577-583.

41.   (a) Min, Y.; Qi, X. F.; Xu, Q.; Chen, Y., Enhanced reactive oxygen species on a phosphate modified C 3 N 4/graphene photocatalyst for pollutant degradation. *Cryst. Eng.Comm.* **2014,** *16* (7), 1287-1295; (b) Xiang, Q.; Yu, J., Graphene-based photocatalysts for hydrogen generation. *J. Phys. Chem. Lett.* **2013,** *4* (5), 753-759; (c) Schrinner, M.; Proch, S.; Mei, Y.; Kempe, R.; Miyajima, N.; Ballauff, M., Stable bimetallic gold–platinum nanoparticles immobilized on spherical polyelectrolyte brushes: synthesis, characterization, and application for the oxidation of alcohols. *Adv. Mater.* **2008,** *20* (10), 1928-1933; (d) Upadhyay, R. K.; Soin, N.; Roy, S. S., Role of graphene/metal oxide composites as photocatalysts, adsorbents and disinfectants in water treatment: a review. *RCS. Adv.* **2014,** *4* (8), 3823-3851.

42.   (a) Chemelewski, W. D.; Lee, H.-C.; Lin, J.-F.; Bard, A. J.; Mullins, C. B., Amorphous FeOOH oxygen evolution reaction catalyst for photoelectrochemical water splitting. *J. Am. Chem. Soc.* **2014,** *136* (7), 2843-2850; (b) Friebel, D.; Louie, M. W.; Bajdich, M.; Sanwald, K. E.; Cai, Y.; Wise, A. M.; Cheng, M.-J.; Sokaras, D.; Weng, T.-C.; Alonso-Mori, R., Identification of highly active Fe sites in (Ni, Fe) OOH for electrocatalytic water splitting. *J. Am. Chem. Soc.* **2015,** *137* (3), 1305-1313.

43.   Johnson, J. T.; Panas, I., Water adsorption and hydrolysis on molecular transition metal oxides and oxyhydroxides. *Inorg. Chem.* **2000,** *39* (15), 3181-3191.

44.   Ye, S. H.; Shi, Z. X.; Feng, J. X.; Tong, Y. X.; Li, G. R., Activating CoOOH Porous Nanosheet Arrays by Partial Iron Substitution for Efficient Oxygen Evolution Reaction. *Angew Chem. Int. Ed.* **2018,** *57* (10), 2672-2676.

45.   Subbaraman, R.; Tripkovic, D.; Chang, K.-C.; Strmcnik, D.; Paulikas, A. P.; Hirunsit, P.; Chan, M.; Greeley, J.; Stamenkovic, V.; Markovic, N. M., Trends in activity for the water electrolyser reactions on 3d M (Ni, Co, Fe, Mn) hydr (oxy) oxide catalysts. *Nat. Mater.* **2012,** *11* (6), 550.

46.   Li, M.; Xiong, Y.; Liu, X.; Bo, X.; Zhang, Y.; Han, C.; Guo, L., Facile synthesis of electrospun MFe 2 O 4 (M= Co, Ni, Cu, Mn) spinel nanofibers with excellent electrocatalytic properties for oxygen evolution and hydrogen peroxide reduction. *Nanoscale.* **2015,** *7* (19), 8920-8930.

47.   Corrigan, D. A., The catalysis of the oxygen evolution reaction by iron impurities in thin film nickel oxide electrodes. *J. Electro. Soc.* **1987,** *134* (2), 377-384.

48.   Liu, G.; Gao, X.; Wang, K.; He, D.; Li, J., Mesoporous nickel–iron binary oxide nanorods for efficient electrocatalytic water oxidation. *Nano Res.* **2017,** *10* (6), 2096-2105.

49.   Diaz-Morales, O.; Ledezma-Yanez, I.; Koper, M. T.; Calle-Vallejo, F., Guidelines for the rational design of Ni-based double hydroxide electrocatalysts for the oxygen evolution reaction. *ACS. Catal.* **2015,** *5* (9), 5380-5387.

50.   (a) Burke, M. S.; Zou, S.; Enman, L. J.; Kellon, J. E.; Gabor, C. A.; Pledger, E.; Boettcher, S. W., Revised oxygen evolution reaction activity trends for first-row transition-metal (oxy) hydroxides in alkaline media. *J. Phy. Chem. Lett.* **2015,** *6* (18), 3737-3742; (b) Zou, S.; Burke, M. S.; Kast, M. G.; Fan, J.; Danilovic, N.; Boettcher, S. W., Fe (oxy) hydroxide oxygen evolution reaction electrocatalysis: Intrinsic activity and the roles of electrical conductivity, substrate, and dissolution. *Chem. Mater.* **2015,** *27* (23), 8011-8020.

51.   Padhi, D. K.; Parida, K., Facile fabrication of α-FeOOH nanorod/RGO composite: a robust photocatalyst for reduction of Cr (VI) under visible light irradiation. *J. Mater. Chem. A* **2014,** *2* (26), 10300-10312.

52.   Zhou, M.; Weng, Q.; Zhang, X.; Wang, X.; Xue, Y.; Zeng, X.; Bando, Y.; Golberg, D., In situ electrochemical formation of core–shell nickel–iron disulfide and oxyhydroxide heterostructured catalysts for a stable oxygen evolution reaction and the associated mechanisms. *J. Mater. Chem A.* **2017,** *5* (9), 4335-4342.

53.   Khan, I. A.; Badshah, A.; Nadeem, M. A.; Haider, N.; Nadeem, M. A., A copper based metal-organic framework as single source for the synthesis of electrode materials for high-performance supercapacitors and glucose sensing applications. *Int. J. Hydrog. Energy* **2014,** *39* (34), 19609-19620.

54.   Nadeem, M. A.; Thornton, A. W.; Hill, M. R.; Stride, J. A., A flexible copper based microporous metal–organic framework displaying selective adsorption of hydrogen over nitrogen. *Dalton Trans* **2011,** *40* (13), 3398-3401.

55.   Nguyen, L. T.; Le, K. K.; Truong, H. X.; Phan, N. T., Metal–organic frameworks for catalysis: the Knoevenagel reaction using zeolite imidazolate framework ZIF-9 as an efficient heterogeneous catalyst. *Catal. Sci. Tech.* **2012,** *2* (3), 521-528.

56.   Nadeem, M. A.; Bhadbhade, M.; Stride, J. A., Four new coordination polymers constructed from benzene tricarboxylic acid: synthesis, crystal structure, thermal and magnetic properties. *Dalton Trans.* **2010,** *39* (41), 9860-9865.

57.   Nadeem, M. A.; Craig, D. J.; Bircher, R.; Stride, J. A., Magneto-structural correlations of a three-dimensional Mn based metal–organic framework. *Dalton Trans.* **2010,** *39* (18), 4358-4362.

58.   Sun, D.; Ma, S.; Ke, Y.; Petersen, T. M.; Zhou, H.-C., Synthesis, characterization, and photoluminescence of isostructural Mn, Co, and Zn MOFs having a diamondoid structure with large tetrahedral cages and high thermal stability. *Nat. commun.* **2005,** (21), 2663-2665.

59.   Ehrenmann, J.; Henninger, S. K.; Janiak, C., Water Adsorption Characteristics of MIL-101 for Heat-Transformation Applications of MOFs. *Eur. J. Inorg. Chem.* **2011,** *2011* (4), 471-474.

60.   Eddaoudi, M.; Kim, J.; Rosi, N.; Vodak, D.; Wachter, J.; O'keeffe, M.; Yaghi, O. M., Systematic design of pore size and functionality in isoreticular MOFs and their application in methane storage. *Science* **2002,** *295* (5554), 469-472.

61.   Czaja, A. U.; Trukhan, N.; Müller, U., Industrial applications of metal–organic frameworks. *Chem. Soc. Rev.* **2009,** *38* (5), 1284-1293.

62.   Canivet, J.; Fateeva, A.; Guo, Y.; Coasne, B.; Farrusseng, D., Water adsorption in MOFs: fundamentals and applications. *Chem. Soc. Rev.* **2014,** *43* (16), 5594-5617.

63.   Li, X.; Hu, Y.; Wang, Z., Investigation of dislocation structure in a cyclically deformed copper single crystal using electron channeling contrast technique in SEM. *Mater. Sci. Eng A.* **1998,** *248* (1-2), 299-303.

64.	Thust, A.; Coene, W.; De Beeck, M. O.; Van Dyck, D., Focal-series reconstruction in HRTEM: Simulation studies on non-periodic objects. *Ultramicroscopy* **1996,** *64* (1-4), 211-230.

65.	Vander Wal, R. L.; Yezerets, A.; Currier, N. W.; Kim, D. H.; Wang, C. M., HRTEM Study of diesel soot collected from diesel particulate filters. *Carbon* **2007,** *45* (1), 70-77.

66.	De Beeck, M. O.; Van Dyck, D.; Coene, W., Wave function reconstruction in HRTEM: the parabola method. *Ultramicroscopy* **1996,** *64* (1-4), 167-183.

67.	Golberg, D.; Bando, Y.; Bourgeois, L.; Kurashima, K.; Sato, T., Large-scale synthesis and HRTEM analysis of single-walled B-and N-doped carbon nanotube bundles. *Carbon* **2000,** *38* (14), 2017-2027.

68.	Romano, A.; Vanhellemont, J.; Bender, H.; Morante, J., A fast preparation technique for high-quality plan view and cross-section TEM specimens of semiconducting materials. *Ultramicroscopy* **1989,** *31* (2), 183-192.

69.	Futian, H.; Lingbo, H.; Shiquan, Z.; Renmao, B., THE STUDY OF CDF ANALYSIS METHOD AND ITS PROGRAM [J]. *Poly. Mater. Sci. Eng.* **1994,** *3*.

70.	Hovius, R.; Vallotton, P.; Wohland, T.; Vogel, H., Fluorescence techniques: shedding light on ligand–receptor interactions. *Trends in pharmacological sciences* **2000,** *21* (7), 266-273.

71.	Moore, D. M.; Reynolds, R. C., *X-ray Diffraction and the Identification and Analysis of Clay Minerals*. Oxford university press: Oxford: 1989; Vol. 322.

72.	Lichtenberger, D. L.; Kellogg, G. E., Characterization of Metal Complex Positive Ions in the Gas Phase by Photoelectron Spectroscopy. In *Gas Phase Inorganic Chemistry*, Springer. 1989; pp 245-277.

73.	Watts, J. F.; Wolstenholme, J., An introduction to surface analysis by XPS and AES. *An Introduction to Surface Analysis by XPS and AES, by John F. Watts, John Wolstenholme, Wiley-VCH, May.* **2003**, *pp,* 224.

74.	Franinović, M., X-ray photelectron spectroscopy.

75.	Reinert, F.; Hüfner, S., Photoemission spectroscopy—from early days to recent applications. *J. Phy.* **2005,** *7* (1), 97.

76.	Evans, D. H.; O'Connell, K. M.; Petersen, R. A.; Kelly, M. J., Cyclic voltammetry. ACS. Pub. 1983.

77.	Harnisch, F.; Freguia, S., A basic tutorial on cyclic voltammetry for the investigation of electroactive microbial biofilms. *Chemistry–An Asian Journal* **2012,** *7* (3), 466-475.

78.   Horkans, J., The hydrogen region of the cyclic voltammetry of Pd: the effect of pH and anion. *J. Electro. Chem.* **1986,** *209* (2), 371-376.

79.   Villar-Rodil, S.; Paredes, J. I.; Martínez-Alonso, A.; Tascón, J. M., Preparation of graphene dispersions and graphene-polymer composites in organic media. *J. Mater. Chem.* **2009,** *19* (22), 3591-3593.

80.   Shinagawa, T.; Garcia-Esparza, A. T.; Takanabe, K., Insight on Tafel slopes from a microkinetic analysis of aqueous electrocatalysis for energy conversion. *Sci. Rep.* **2015,** *5*, 13801.